Temperature Swing Adsorption Using Amine Impregnated Adsorbent for CO_2 Capture

By

SAHIL BANGAR

A thesis submitted in partial fulfillment of the requirements for the degree of

Master of Science

in

Chemical Engineering

Department of Chemical and Materials Engineering
University of Alberta

Abstract

Capture of carbon dioxide from flue gas using amine functionalized silica based adsorbents has shown great potential recently. Despite their stable performance, the full potential of these adsorbents has not been researched in greater depth. In this thesis, experimental study and simulation of a temperature swing adsorption process for capture of CO_2 and regeneration of the adsorbent using steam were carried out. Special emphasis was given on maximizing the purity of CO_2 captured using this process, so as to lower the cost of further compression required for sequestration.

For simulation of the cyclic temperature swing adsorption process, experimental measurements were carried out to study the adsorbent, suitable process modeling software was chosen and cycle configurations to maximize the performance of adsorbent were developed. Experimental isotherm data was collected for the amine impregnated adsorbent and an isotherm model was fitted. Subsequently, the isotherm parameters from the fitted model were used as input data for modeling of cyclic TSA processes. A reliable adsorption process simulator was then chosen based on its ability to accurately predict the column dynamics for an adsorption process. Model equations for the one-dimensional rigorous model comprising of mass, momentum and heat balances used for the simulation of the adsorption process are detailed. The effective model predictions of the simulator were validated using an adsorption process described in the literature, since the results were discerned to be in the acceptable range, further simulations using the software were carried out.

A basic 3-step TSA cycle was developed to capture CO_2 using amine impregnated silica adsorbent. Since the purity of the CO_2 recovered using this configuration was not very high, another 4-step cycle with steam purge was implemented. The introduction of the steam purge step improved the purity considerably while lowering the

recovery marginally. Parametric studies for both the cycles were also performed to determine the best operating conditions for the process.

Acknowledgements

I could not have completed this thesis without the help of many people. Foremost, I would like to thank my supervisor, Dr. Rajender Gupta, for helping me transition from an immature student to a developed researcher. His patience and determination are truly admirable and it was due to his confidence, guidance and support in my abilities that I could go further than I thought was possible. I would also like to thank Dr. Arvind Rajendran, for providing his expertise and suggestions in key areas of this project. Arvind, you'll always be a source of professional inspiration for me.

I am grateful to Dr. Deepak Pudasianee for his valuable suggestions and assistance at various stages of this work. I am also thankful to all members of the C^5MPT lab for their kind cooperation thoughout my program. I would like to especially thank my colleague, Navjot Kaur Sandhu for her technical assistance during the course of my research work.

I am indebted to my many student colleagues for providing a stimulating and fun environment in which to learn and grow. I am especially grateful to Rishik Ranjan, for helping me understand the working of the software without even being related to it, Rahul Raveendran, for providing sound advices to my many qualms, Vinoj Kurian, for encouraging me to push harder and effortlessly showing me the right path to take, Satarupa Dhir, for taking out time and helping me clear my chemical engineering fundamentals, Komal Dhankar, for always encouraging me, Ankit Kumar, for transforming me into a healthier individual both physically and mentally, Deepesh Kumar, for all the good times and for his much valued timely consultations, Shantanu Patel for helping me pass through the toughest phase of my life, I offer my profoundest gratitude. Lastly, I would like to thank Vinayak R. Narulkar for being very kind in

providing invaluable advices pertaining to my growth into a professional individual.

I would also like to thank Ashwin Kumar Rajagopalan (a.k.a Mastermind). Throughout my research and thesis-writing period, he provided encouragement, sound advice, good teaching, and lots of great ideas. I would have been lost without him.

I am grateful for having a loving family. I thank, my late maternal grandparents, for showering their blessings on me and paternal grandparents, for enabling me to achieve everything in life so far. My sister, Sonali has always showed me the definitions of courage and achievement. I thank my parents, Madan Lal and Paramjeet, for inspiring me to pursue my love for science and supporting me through all of life's ups and downs.

Contents

List of Figures

List of Tables

Chapter 1

Introduction

1.1 Background

With effects of global warming becoming more and more prevalent, carbon dioxide (CO_2) has come under spotlight because of its contribution as the primary greenhouse gas and its consequences on climate change. With the dawn of industrial revolution, large amounts of CO_2 has been added into the atmosphere primarily due to the burning of fossil fuels, deforestation which liberates the CO_2 stored in the trees and also the processing of various chemicals. The result of this rapid growth and exploitation of natural resources has increased the CO_2 concentrations in the Earth's atmosphere. The climate change we observe daily is due to the surplus CO_2 in the atmosphere which has now become an immediate threat to our prosperity and existence as living beings on this planet.

Atmospheric CO_2 concentrations have increased to almost 400 ppm (parts per million) [25] which is a growth of more than 100 ppm since its pre-industrial levels in a matter of 300 years. Thirteen out of the last fourteen years (2000-2014) have been the warmest years in the instrumental record of global surface temperature (since 1850) with 2014 being the warmest year in modern record [39]. The alarmingly increasing linear warming trend shows that the increase in temperature over the last 50 years from 1956 to 2005 is nearly twice that for the 100 years from 1906 to 2005 as shown in Figure 1.1. Since CO_2 is the most crucial anthropogenic greenhouse gas in causing global warming, there is unquestionable correlation between the alarming tempera-

ture increase and the atmospheric CO_2 concentrations.

According to a recent forecast [4] for the period 2004-2030 the global energy demand is bound to increase by 53% which would result in a 55% increase in global CO_2 emissions. Fossil fuels would be the prime source of energy providing for 83% increase in the energy needs; and power generation would be responsible for almost 44% of global CO_2 emissions by 2030 as the demand for electricity increases. If not mitigated now, the increasing CO_2 levels can cause catastrophic events which include but not limited to rise in ocean levels, dislocation of human settlements, extreme weather events: higher frequency of heat waves, storms and irregularities in rainfall patterns causing droughts and floods [77]. End result of all this would be food shortage, increased human diseases and ailments and finally mortality.

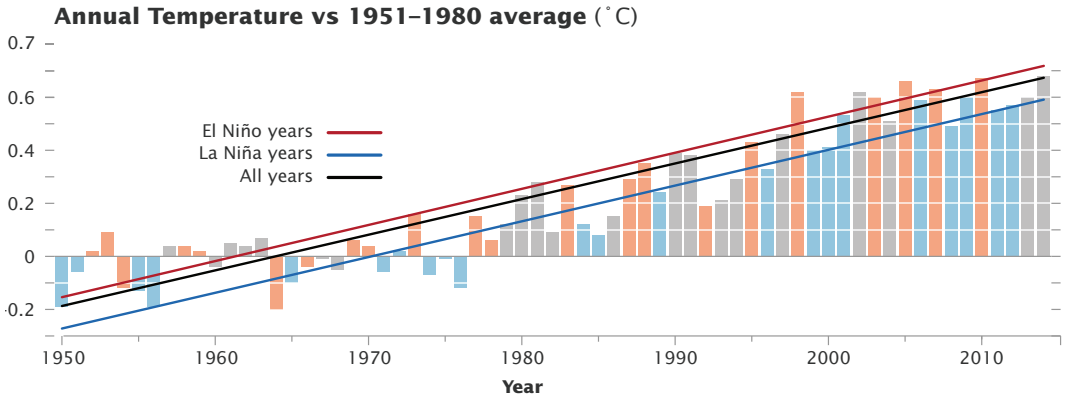

Figure 1.1: Temperature anomalies for 1950-2014. Source: NASA: Goddard Institute of Space Studies [40]

There is an urgent need to reduce the global CO_2 emissions in the near future which makes the need to capture CO_2 a necessity for greenhouse gas reduction. Therefore, the agenda on global wide cooperation in CO_2 reduction without compromising our economic growth, security and living standards has been explicitly put forward from a standpoint of long term sustainable development. Keeping in mind recent developments in CO_2 capture technologies, there is a wide scope for improvement in their existing applications to capture CO_2 from power plants which would mitigate the largest source of greenhouse gas emissions.

1.2 Carbon Capture Technologies

Fossil fuels are irreplaceable for the technological advancements in this century because of their energy density, enormous resource reserves and established infrastructure for exploitation and production [73]. A world without fossil fuels for generation of heat and power, and for use in heavy industrial manufacturing operations is not feasible as of now nor in the foreseeable future.

In the wake of such demand for fossil fuels along with need to reduce CO_2 emissions, Carbon Capture and Storage (CCS) technologies are a promising route to achieving a meaningful reduction in CO_2 emissions in the near-term. Reduction of emissions from anthropogenic point sources by 80-90% are consistently discussed as achievable targets by CCS technologies. The challenges posed by the transport and storage of such large quantities of captured CO_2 are perplexing but are certainly not impossible. The methods selected for CO_2 capture should be feasible not only economically and socially but also environmentally as it makes little sense in consuming resources to eradicating one problem, while consequently generating another. Three basic CCS technology options shown in Figure 1.2 are generally envisaged as being suitable for commercial deployment in the near to medium term:

- Post-combustion capture
- Pre-combustion capture
- Oxy-fuel combustion capture

1.2.1 Post-Combustion Capture

Application Area - Coal and gas-fired plants

This process removes CO_2 from flue gas produced after combustion of fuels (namely, coal, natural gas and biomass). The flue gas produced is at atmospheric pressure with a less than 15% concentration of CO_2 for coal-fired and as low as 4% for gas fired plants [68]. This poses a major challenge for CO_2 capture using this process as the energy penalty and other costs for further concentration of CO_2 (above 95.5%) for transportation and storage are escalated manifolds [79].

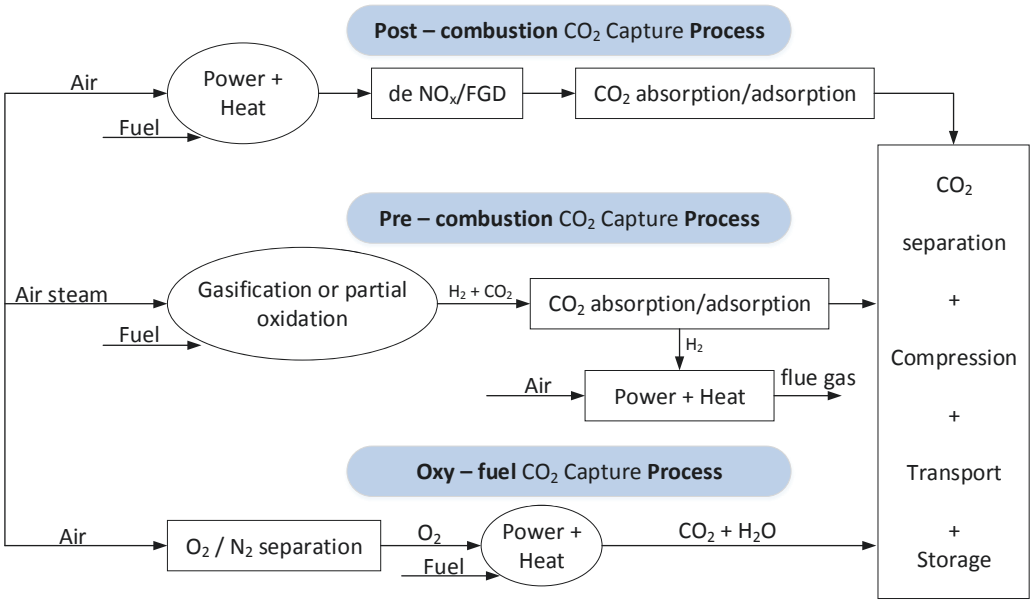

Figure 1.2: Carbon capture and storage technologies. Adapted from [68]

Some of the pros and cons of the process are listed below.

Advantages

- Mature technology as compared to other processes, with easy integration into existing plants [68]
- Similar concepts deployed in several industries worldwide [73]
- Proven demonstration of technology already in existence, such as 110MW Boundary Dam project by SaskPower in Canada.

Technical Challenges

- Very energy consuming process during solvent regeneration.
- Solvent susceptible to degradation in the presence of oxygen requiring continuous replenishment. [73], [79]

- High capital and operational costs along with disastrous impacts on the environment.
- Addition of current amine technologies to plants would reduce power output by 30% and efficiency by 11%.

1.2.2 Pre-Combustion Capture

Application area - Coal-gasification plants

In this process the fuel is gasified in low oxygen levels forming syngas (comprising of mainly CO and H_2) which further undergoes water gas shift reaction in the presence of steam to convert CO to CO_2 and more H_2. This process can be easily applied in Integrated Gasification Combined Cycle (IGCC) but would bring down the plant efficiency by 7-8%. Other benefits and constraints are listed below:

Advantages

- Existing technology with very low emissions. Can be retrofitted to existing plants.
- Good sorption efficiency due to high CO_2 concentration.
- Commercially practised at required scale in alternate industrial sectors [68].
- Less energy penalty (about 20%) when compared to post-combustion capture (PCC) (about 30%) with 90% capture efficiency.

Technical Challenges

- Heat transfer issues due to high temperatures involved and the use of hydrogen-rich gas turbine fuel lowers the efficiency of the plant [68].
- High energy penalty for sorbent regeneration.
- Few IGCC plants in operation worldwide which would add to inadequate experience and application issues [36].

- High capital and operating costs.

1.2.3 Oxy-fuel Combustion Capture

Application area - Coal and gas-fired plants

As the name suggests, in this process combustion of fuel takes place in the presence of excess of oxygen instead of air. This reduces the amount of nitrogen present in the exhaust gas which lowers the level of thermal NO_x substantially along with making the CO_2 separation process easier. Though the process is very attractive and feasible, the generation of large amounts of oxygen requires use of a very energy intensive air separation unit. The costs and energy penalty are increased by more than 7% when compared to a plant without CCS technology [11]. Other benefits and constraints are listed below:

Advantages

- CO_2 produced is of very high concentration, improving the overall capture efficiency.
- Relatively simple technology with suitability to be retrofitted with existing plants.
- Mature air separation technologies needed are already in operation.
- Volume of gas to be handled is reduced significantly; thus, requiring smaller equipments which are commercially available [68].

Technical Challenges

- May cause excessive corrosion due to presence of high CO_2 and SO_2 concentration.
- Production of cryogenic O_2 is costly [68].
- Combustion in oxygen is cumbersome and may add to complications in the

process [79].

- New technology, needs to be demonstrated on a commercial scale.

Handling of large volumes of flue gas produced at atmospheric pressures in post-combustion process is the most challenging aspect of the technology. On comparison with pre-combustion capture which is limited in application to new power plants due to the required modifications in combustion process, post-combustion capture is more promising. And as discussed earlier, separation of oxygen from air is an energy intensive and expensive process, rendering oxy-fuel to be developed more at this stage. Figure 1.3 outlines the current status of the technologies along with their level of maturity for deployment to industrial sector. At this stage, due to economical, social, technological and environmental reasons PCC of CO_2 seems to be the most reasonable technology to be integrated with existing power plants.

		Syngas-hydrogen capture	*Post-process capture*	*Oxy-fuel combustion*	*Inherent separation*
First-phase industrial applications	Gas	-	-	-	Sweetening
	Iron and steel	Direct reduced iron (DRI), smelting (*e.g.* Corex)	-	-	DRI
	Refining	-	-	-	Coal-to-liquids; synthetic natural gas from coal
					Hydrogen production
	Chemicals	-	-	-	Ammonia/methanol
	Biofuels				Ethanol fermentation
Power generation	Gas	Gas reforming and combined cycle	Natural gas combined cycle	Oxy-fuel combustion	Chemical looping combustion
	Coal	Integrated gasification combined cycle (IGCC)	Pulverised coal-fired boiler	Oxy-fuel combustion	Chemical looping combustion
	Biomass	IGCC	Biomass-fired boiler	Oxy-fuel combustion	Chemical looping combustion
Second-phase industrial applications	Iron and steel	Hydrogen reduction	Blast furnace capture	Oxy-fuel blast furnace	-
	Refining	Hydrogen fuel steam generation	Process heater and combined heat and power (CHP) capture	Process heater and CHP oxy-fuel	-
	Chemicals	-	Process heater, CHP, steam cracker capture	Process heater and CHP oxy-fuel	-
	Biofuels	Biomass-to-liquids	-	-	Advanced biofuels
	Cement	-	Rotary kiln	Oxy-fuel kiln	Calcium looping
	Pulp and paper	Black liquor gasification	Process heater and CHP capture	Process heater and CHP oxy-fuel	-

Commercial Demonstration Pilot Lab or concept

Legend: technical maturity of operational CO_2 capture plants to date.

Figure 1.3: Routes to CO_2 capture in power generation (by fuel) and industrial applications (by sector). Recreated from [5].

1.3 CO_2 Separation Technologies for Post-Combustion Capture

Even though, there is a worldwide consensus that PCC is the closest technology to be implemented in order to abate anthropogenic CO_2 emissions, lack of incentive that is appreciably rewarding for industries to perform CO_2 reduction is inadequate [68]. The high cost of CO_2 capture , particularly from dilute streams like those from coal and gas fired plants, steel and iron manufacturing plants, cement kilns and IGCC plants is the single limiting factor for implementation of this technology. The composition and amount of the flue gas emerging from different sources as shown in Table 1.1 is also not the same, thus imposing further limitations of the potential of the technology. The performance of the technology in presence of SO_x, NO_x and and other pollutants is still not clear and requires further R&D to make the process possible without additional pre-treatment of the flue gas prior to capture.

Table 1.1: Flue gas composition from various industrial processes [77] [89]

Process	**CO_2 (dry) vol%**	**Pressure of gas stream (MPa)**	**Impurities**
Coal fired boiler	12-14	0.1	High SO_x and NO_x levels, O_2: 2-5%
Gas fired boiler	7-10	0.1	Low SO_x and NO_x levels
Gas turbine exhaust	3-4	0.1	Low SO_x and NO_x levels, O_2: 12-15%
Blast furnace gas: post combustion	27	0.1	SO_x and NO_x present
Cement furnace off-gas	14-33	0.1	SO_2 and NO_x, trace elements, particulates
Natural gas processing	2-65	0.9-8	SO_x and NO_x present
IGCC syngas: post-gasification	8-20	2-7	SO_x and NO_x present

1.3.1 Absorption

Post-combustion capture of CO_2 by absorption/stripping technology, using 20-30 wt% amine solutions such as monoethanolamine (MEA)/diethanolamine (DEA), is a commercialized technology used in the industry for 60 years and is regarded as the most mature technology [79]. The schematic representation of the capture system and reaction mechanism by which MEA removes CO_2 from combustion flue gas stream are shown in Figure 1.4. MEA solution comes in contact with the flue gas in an absorber column where absorption of CO_2 by the solution takes place. In a commercial process, flue gas is bubbled through the solvent in a packed absorber column, where CO_2 is preferentially removed from the flue gas by the solvent. The CO_2 rich solvent then passes through a regeneration unit, where the absorbed CO_2 is stripped from the solvent by counter-flowing steam at $100 - 200^oC$ [79]. This process of separating CO_2 by steam is termed as stream stripping. The water vapours are then condensed, resulting in a highly concentrated (over 99%) CO_2 stream, which can be compressed for commercial utilization or for storage. The lean solvent is then cooled to $40 - 65^oC$ and is recycled back into the absorber column. According to the mechanism shown in Figure 1.4, the majority of the captured CO_2 results in the formation of bicarbonate in the process. 2 mol-amine/mol-CO_2 are required in aqueous media for the formation of stable bicarbonate compounds resulting in the capture of CO_2.

The absorption process suffers the following disadvantages for CO_2 separation from flue gases [35], [84], [111]:

1. Low loading capacity (g of CO_2 absorbed/g of absorbent) of the solvent.
2. Regular equipment replacement due to high corrosion rates.
3. Degradation of the amine in the presence of SO_x, NO_2, HCl and HF and O_2. This increases the consumption of the absorbent leading to a high absorbent make-up rate. In case of capturing CO_2 from flue gas of coal fired plants, the MEA process cannot be used prior to removal of SO_2 from the flue gas stream since MEA undergoes oxidative degradation forming irreversible products.

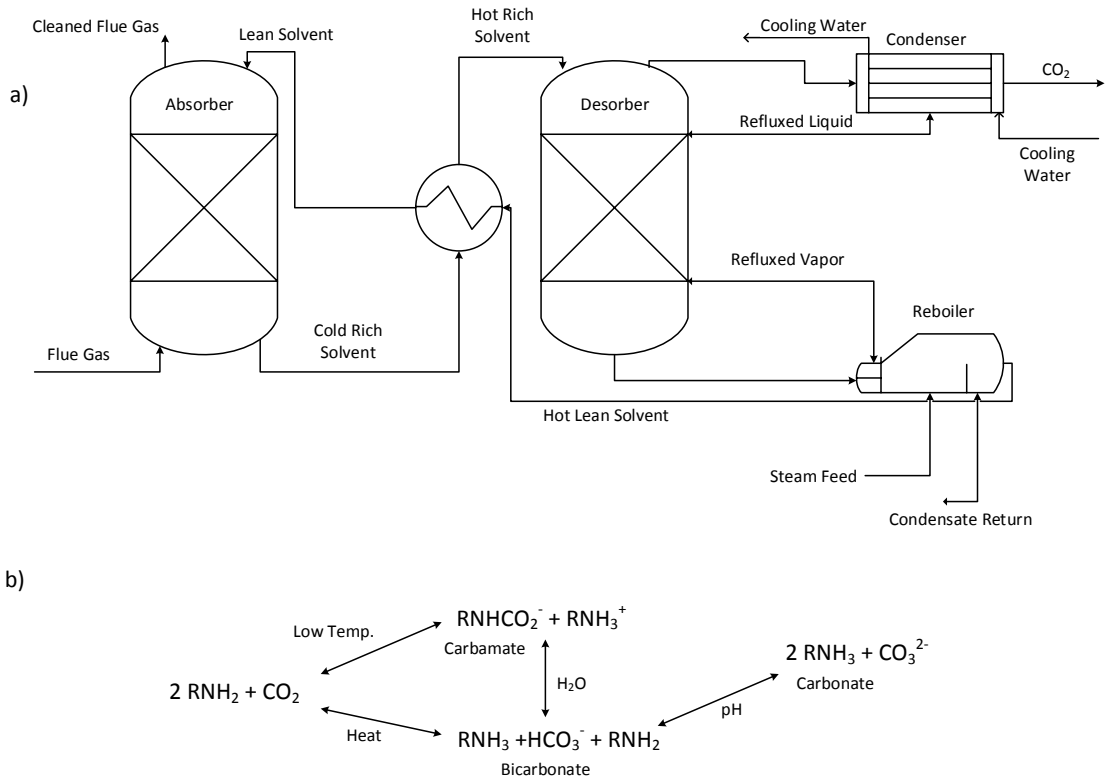

Figure 1.4: a) Basic chemical absorption process for amine based CO_2 capture, b) Proposed reaction mechanism for capture of CO_2 by liquid amine based system. Adapted from [73] and [89] respectively.

4. Regeneration of the absorbent requires large amounts of energy to achieve high regeneration temperatures of the process.

By and large, opportunities for process and solvent improvements exist and can be made possible by focused R&D. Meanwhile, alternative technologies are gaining lot of interest and attention, one such technology is adsorption for CO_2 capture.

1.3.2 Adsorption

Solid adsorbents for CO_2 capture are in the early stage of development and are forseen as one of the many promising CO_2 capture technologies. Some key advantages of solid sorbents over other CO_2 capture options, including aqueous amines, are as follows [102] [97]:

1. Energy penalty reduction
    - Latent heat reduction from H_2O evaporation
    - Deployment of heat recovery will reduce sensible heat requirement
2. Negligible corrosion
    - Corrosion inhibitors are not required
    - Lack of corrosive environment allows for less expensive and sophisticated construction materials to be utilized
3. Potentially hazardous emissions control
    - Amine emissions are reduced
4. Water savings
    - Reductions in cooling water requirements
    - Negligible liquid waste
5. Lesser operational problems
    - Lack of foaming or other liquid-related operation concerns

In general, solid adsorbents used for CO_2 capture can be broadly classified into: a) Physisorbents and b) Chemisorbents.

Carbon-based materials, zeolites and metal organic frameworks (MOFs) mainly make up the class of physisorbents. Chemisorbents mainly comprise of solid sorbents obtained through addition of specific functional groups (basic) which enhance chemical reaction effect between CO_2 molecules (acidic) and adsorbents. Adsorption based capture cycle of CO_2 can be further classified on the method employed to regenerate the sorbent. Studies on various regeneration techniques are, pressure swing adsorption (PSA), temperature swing adsorption (TSA), elctrothermal swing adsorption (ESA), vacuum swing adsorption (VSA) and hybrid variants (VPSA, TVSA, TPSA) have been carried out. The basis of technique selection include, type of adsorbent, sorbent CO_2/N_2 selectivity, and working capacity depending on temperature and pressure.

With the boom in emergence of new materials for CO_2 capture, screening , evaluation and selection of the best sorbent is of prime importance. The key criteria for selecting an adsorbent for CO_2 capture has been listed below:

- *High adsorption capacity of CO_2:* Equilibrium adsorption capacity, defined as the maximum amount of a component (CO_2 in our case) that can be adsorbed by the adsorbent at a given capture condition, is the most crucial factor in determining the capability of an adsorbent to be screened for capturing CO_2. Adsorption capacity is of paramount importance to the capital cost as it governs the quantity of adsorbent required, which also fixes the volume of the adsorber column, and together these factors are generally significant if not dominant. The ideal adsorbent should exhibit a steep slope (preferential) CO_2 adsorption isotherm at low CO_2 partial pressures implying a high uptake of CO_2 by the adsorbent. Ideal sorbents should be able to operate at less than 0.4 bar CO_2 partial pressure with a total gas pressure of 1-2 bar and temperature of about $70 - 80^oC$. Attaining equilibrium can be a time intensive process and thus working capacity is used instead. Working capacity is the difference in adsorption capacities at the operating and regenerating temperatures or pressures, depending on the technique used. To be comparable with amine-based absorption process, an optimum adsorbent for capture of CO_2 from flue gas, must exhibit a CO_2 adsorption capacity of 2-4 mmol of CO_2/g of adsorbent [54].

- *High selectivity of CO_2:* Flue gas contains many other components apart from CO_2, therefore the adsorbent should preferentially adsorb CO_2 over bulk gas components present. Adsorbent with high selectivity towards CO_2 would produce high purity product stream requiring less processing before compression for storage.

- *Fast adsorption/desorption kinetics:* The adsorbent should be capable of rapidly adsorbing and desorbing CO_2 allowing for short cycle times. Adsorption kinetics affects the working capacity of the adsorbent, which in turn determines the amount of CO_2 captured. Fast kinetics are indicated by sharp fronts at the onset of both adsorption and desorption. Mass transfer, diffusional resistances

of gas phase through the sorbent and the reaction kinetics of CO_2 with present functional groups are the main factors influencing the rate of adsorption.

- *Mechanical strength/ multiple cycle stability:* Operational life of adsorbents, which determines the replacement frequency of the adsorbent is also very crucial as it affects the economics when considered on a commercial scale. Adsorbent should be able to perform adsorption and desorption over several continuous cycles, without any significant loss in its adsorption capacity or kinetics. Adsorbent must be resistant to crushing and abrasions occurring within the adsorber vessels. Change in the operational conditions (temperature or pressure), variable flow rates and vibrations should not affect the performance of the sorbent both morphologically (support) or chemically (degradation or leaching of functional groups).

- *Tolerance to impurities:* Impurities such as SO_x, NO_x, O_2, moisture, fly ash and heavy metals are common components with variable concentrations (Table1.1) in flue gas. Affinity and tolerance threshold to these components are properties that directly impact the CO_2 adsorption capacity and selectivity, and thus decide if any upstream flue gas treatment is necessary. Such treatments add to costs and affect the overall economics of the plant. Physisorbents like zeolites have a strong affinity towards moisture which decreases their adsorption capacity considerably. This is not the case with most amine functionalized adsorbents which have proven tolerance and increased adsorption capacity in the presence of moisture [94]. Still the impact of SO_x, NO_x and O_2 on these adsorbents has not been researched in depth.

- *Regeneration:* Optimum interactions between CO_2 and adsorbent should be neither too weak nor too strong. Too weak bonding may result in easy regeneration but would also cause low CO_2 adsorption capacity at low pressures. Conversely, strong affinity results in high adsorption capacity but very difficult and costly desorption. A heat of regeneration substantially lower than the amine scrubbing process is mostly desired so as to overcome the drawbacks of that technology. The heat of regeneration lies in the order of -25 to -50 kJ/mole of CO_2 for

physisorbents and within -60 to -90 kJ/mole of CO_2 for chemisorbents [89].

- *Cost of the material:* This is another important parameter to be considered in the development of any potential adsorbent. Since development of most of the materials is very recent, little information on techno-economic assessment of these materials for commercial scale plants is available. In a economic sensitivity analysis performed by Tarka et al. [103] it was determined that when using a base case cost of \$10/kg of adsorbent, a \$5/kg would prove to be financially favourable and a \$15/kg would turn out to be uneconomical.

It should be noted that although a hypothetical, ideal adsorbent is described above, in reality no single ideal adsorbent is likely to have all the properties in one. Rather, based on the context of application for efficient CO_2 separation, each adsorbents strengths and weaknesses must be considered. Ultimately, large scale commercial adsorbents will be those that perform effectively within a practical and efficient CO_2 separation process. To this end, the behaviour of some of the known classes of adsorbents used for post combustion CO_2 capture along with the adsorption technologies have been reviewed and classified in the next chapter.

1.4 Objectives and Outline of the Thesis

1.4.1 Objectives

The prime objective of this thesis is to study CO_2 capture from flue gas using temperature swing adsorption. Amine-impregnated adsorbents due to their easy synthesis, high CO_2 adsorption capacity, high selectivity towards CO_2 over other impurities and because of their stable performance on exposure to steam, would be studied in this thesis. Thermal stability and stable performance in steam environment are key properties of the synthesized adsorbent, desired for multiple cycles of TSA. The temperature swing is to be performed using steam, due its easy separation with the captured CO_2 and also determine the best possible process configuration in which the purity and recovery of CO_2 can be maximized. This study to capture CO_2 and regenerate the adsorbent using steam, includes the experimental investigation of the

adsorbent material, to determine the adsorption isotherm parameters for the modeling of the cyclic process of TSA.

The major objectives of this study are:

- To measure the single-component adsorption isotherms experimentally at different temperatures for the amine impregnated sorbent and study its performance in a simulated cyclic process.
- To screen and select a suitable simulator capable of modeling temperature swing adsorption cycles.
- To test different TSA configurations for maximizing purity and recovery of the CO_2 capture process. Furthermore, to study the effect of different parameters like step times and bed length on purity and recovery.

1.4.2 Thesis Outline

Chapter 1 provides a broad outlook on the need for CO_2 capture and summarizes the major technologies available for its mitigation. The pros and cons of the potential technologies are discussed and new technologies like adsorption are introduced. The desired traits of a suitable adsorbent material are also provided.
Chapter 2 compiles the literature survey on various types of amine based adsorbents, such as amine functionalized: impregnated and grafted adsorbents used for CO_2 capture. Further, the various types of adsorption/desorption techniques commonly used for CO_2 capture applications are discussed with precedence given to the steam regeneration method.
Chapter 3 illustrates the experimental investigation of the amine impregnated adsorbent. The single component adsorption isotherms were measured experimentally at different temperatures and partial pressures. The measured experimental data was then fitted to an isotherm model. Further, the heat of adsorption for the material was measured using Van't-Hoff equation and determined value was used as an initial guess for the fitting of the isotherm model. Isotherm parameters were then determined by the fitted isotherm model to be used as an input for further cyclic processes.

Chapter 4 presents the simulator used for modeling the cyclic adsorption process. The model equations for the mass, momentum and heat balances to be used for the capture of CO_2 from flue gas are explained in detail in this chapter. The validation of the simulator using an adsorption model from literature is then exhibited.

Chapter 5 deals with the design and implementation of two TSA cyclic configurations, namely, the basic 3-step cycle and the 4-step cycle with steam purge. The purity and recovery of the strongly adsorbed species is studied in this chapter for the two cycles. The effect of different step times and bed length on purity and recovery of the two cycles has also been presented. Chapter 6 concludes the thesis by summarizing the key findings from the experimental studies, simulation and energy estimation. The recommendations and future work in this area are also discussed.

Chapter 2

Literature Review

2.1 Background

Our group has been actively involved in the synthesis, characterization, testing and optimization of amine based solid adsorbents for application in post-combustion CO_2 capture previously [116] [90]. The main aim of this study is to evaluate the performance of amine impregnated silica based adsorbent with regeneration using steam. Keeping in focus the objectives of this study, the literature has been segregated into two broader fields of amine based adsorbents and different adsorption separation processes based on regeneration methodology used.

This chapter describes the various types of amine based sorbents that are currently being studied for CO_2 capture applications. A comprehensive review of the amine functionalized: grafted and impregnated adsorbents has been presented. Furthermore, the various adsorption techniques have been discussed and the work done both experimentally and using modeling in their particular domains has been elaborated. Finally, the motivation and objectives for performing this study are outlined.

2.2 Amine Functionalized Adsorbents

As discussed earlier, CO_2 capture from flue gas by absorption and stripping mechanisms using aqueous amines is a feasible and mature technology. Due to the shortcom-

ings and inherent problems discussed in detail in the previous chapter, research focus has shifted to development of amine-based solid adsorbents by immobilizing organic amines on certain support materials. Low capital costs, pressure for gas recovery and low energy requirements as compared to aqueous amines have made amine-based solid adsorbents an attractive and worthwhile area of consideration [105]. When compared to physisorbents such as zeolites, activated carbons (ACs), metal organic frameworks (MOFs) and carbon nanotubes (CNTs), these materials possess higher selectivity and adsorption capacity for CO_2 at relatively lower pressures.

With respect to amine-based solid sorbents research is motivated to improve CO_2 capture capabilities of these materials by [105]:

1. High amine-loading bearing supports
2. High density amines
3. Stable amine immobilization

The supports must display strong affinity towards amine molecules, high surface area and porosity to facilitate adsorption and material stability and mechanical strength for applications in commercial settings. There are three types of amine based solid adsorbents in general:

1. Class 1: Amine impregnated porous solid sorbents, prepared by physically loading monomeric or polymeric amine species over porous solid support, typically porous silica. It should be noted that no chemical reaction takes place between amine group and the support material.
2. Class 2: Amine grafted porous solid support, in which silane facilitates the covalent bonding of the amines to the solid support. The attachment is accomplished by binding amines to oxides using either silane chemistry or preparing polymeric supports with amine-containing side chains. The strong connection between amine group and support in amine grafted as compared to amine impregnated solid sorbents, makes them more desirable for long-term applications.
3. Class 3: Hybrid of the above classes.

The structure of widely used amines for solid sorbent functionalization are shown in Figure 2.1 [16].

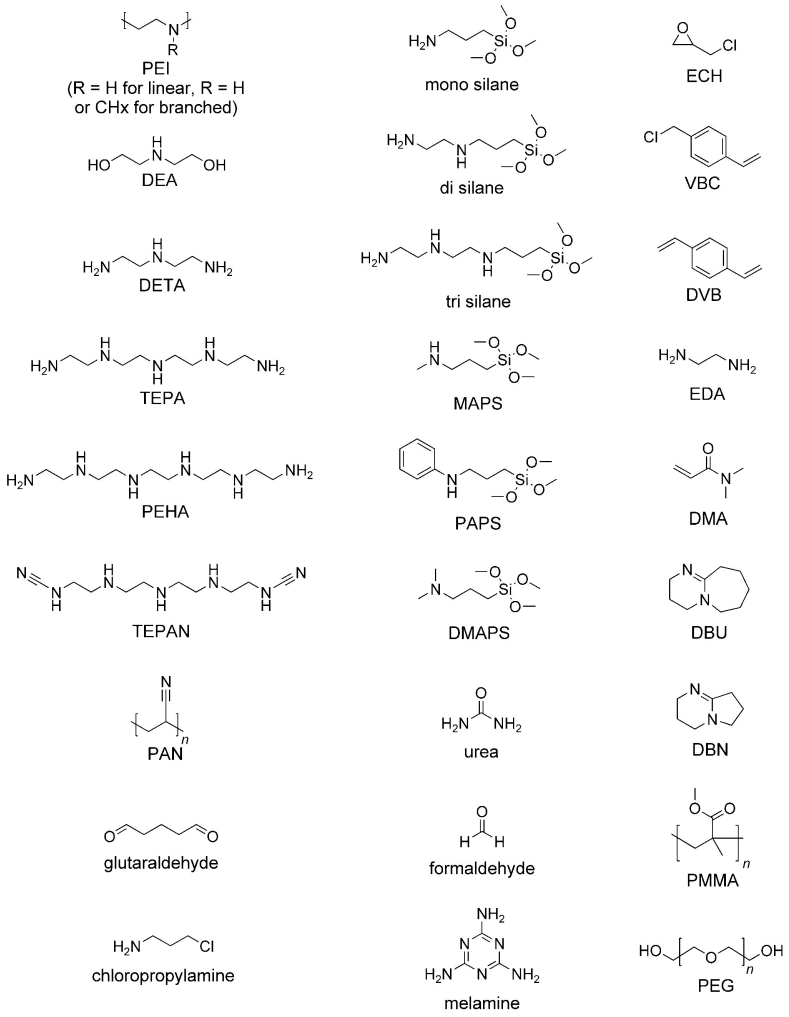

Figure 2.1: Amines, silanes, monomers, and polymers used in the synthesis of solid supported amine adsorbents
Reprinted with permission from Copyright (2009) John Wiley and Sons

2.2.1 Amine Impregnated Adsorbents

Xu et al. [109] was the first to use amine-impregnated silica to capture CO_2. The designed adsorbent was prepared by impregnation of high surface area hydrothermally synthesized mesoporous silica support MCM-41 with polyethyleneimine (PEI) and termed as "molecular basket". MCM-41 prepared using the technique was shown to display a synergistic effect on adsorption of CO_2 on PEI. Reportedly, the adsorption

capacity of the designed adsorbent increased 24 times more than that of MCM-41 and 2 times than that for PEI. They later (in 2003) [110] reported their highest adsorption capacity of 3.02 mmol/g for impregnated sorbent containing 50 wt% PEI loading at 75^{o}C. Uniform dispersion of PEI into the support pores was a critical step in sorbent preparation which lead to this behaviour.

More recently, Ma et al. [72] developed a nanoporous SBA-15-supported sorbent with 50 wt% PEI loading. The sorbent had a sorption capacity of 3.18 mmol/g at 75^{o}C and for a partial pressure of 15 kPa for CO_2. Due to the higher pore diameter and volume of SBA-15, the observed adsorption capacity was 50% more than that of their previously developed MCM-41-PEI adsorbent. Hicks et al. [51] also developed SBA-15 adsorbents impregnated with PEI and Tetraethylepentamine (TEPA). They reported that the TEPA impregnated SBA-15 started to deteriorate in terms of adsorption capacity from second cycle and kept falling in subsequent cycles, owing to leaching of TEPA from the adsorbent surface. In the case of PEI impregnated SBA-15, it was reported that the material became sticky in nature and due to which the adsorbent started clogging the adsorption column which lead to large pressure drop and reduction in volumetric flow rate.

CO_2 adsorption performance was studied for a series of PEI-impregnated (50 wt%) ordered mesoporous silica supports, namely, MCM-41, MCM-48, SBA-15, SBA-16 and KIT-6 by Ahn et al. [100]. All the adsorbents displayed high adsorption capacities, fast kinetic and stability, when compared to pure PEI. The order of adsorption capacities was found to be directly proportional to the order of their average pore diameters and pore arrangement. The CO_2 adsorption capacities were found to be in the following order: KIT-6 (d_p= 6.5 nm) > SBA-15 (d_p= 5.5 nm) > SBA-16 (d_p= 4.1 nm) > MCM-48 (d_p= 3.1 nm) > MCM-41 (d_p= 2.1 nm), where d_p represents the average pore diameter (in nanometers).

Qi et al. [83] proposed a novel high efficiency nanocomposite CO_2 capture platform obtained using PEI and TEPA to functionalize mesoporous silica capsules. the adsorption capacity of the material thus synthesized was reported to be up to 7.9 mmol/g under humidified 10% CO_2 in flue gas. Larger particle size, higher interior void volume and thinner mesoporous shell thickness contributed to the improved adsorption capacity. PEI impregnated sorbents exhibited good cyclic stability over repetitive

adsorption/regenration cycles (50 cycles) in comparison to TEPA.

Among other supports it was clearly noticed that supports with large pore diameter have higher adsorption capacities [37], [57], [43], [117], [55], [38], [82]. Sayari et al. [92] reported that though the increase in amine loadings result in higher adsorption capacities, it also consequently lead to slower adsorption kinetics and lower CO_2/N_2 ratio. High amine content adsorbents operate poorly at low temperatures, as observed by them, the optimum adsorption capacity might occur at higher temperatures. At higher temperatures of adsorption and desorptopn, the weak affinity between the amine and the porous support may lead to amine leaching, making regeneration conditions an integral consideration and at times a limitation in their application.

Further studies paid attention to factors such as the mode of regeneration and adsorbent operational lifetime during the evaluations of amine-impregnated adsorbents. In a study performed by Drage et al. [28], TSA for PEI-impregnated adsorbent was done using pure CO_2, and it was reported that the working capacity of the adsorbent was 2 mmol/g. Adsorption capacity of the adsorbent was reported to decrease over numerous cyclic run indicating poor operational lifetime of the sorbent. At temperatures above 135^oC stable urea compounds were reported to form due to secondary reaction between CO_2 and PEI leading to the irreversible degradation of the adsorbents. The use of steam as a regeneration gas instead of CO_2 was one of the proposed solution to overcome the problem of thermal degradation in TSA. Apart from TSA, Dasgupta et al. [21] studied a single column five-step PSA option using PEI-funtinalized SBA-15 adsorbent. To improve the CO_2 recovery a strong adsorptive rinse cycle during PSA was suggested.

Sayari et al. [49] researched the degradation of PEI supported materials due to thermal, oxidative or CO_2 induced reasons in much depth. According to them to improve the adsorption performance, one must keep in mind the following considerations:

1. Moderate operating conditions improve the thermal stability of the adsorbent.
2. Moisture tends to improve the CO_2 adsorption capacity.
3. High temperatures and dry CO_2 leads to formation of urea.
4. Direct exposure to carbon free air regardless of temperature leads to fast degra-

dation (mainly oxidative) of the adsorbent.

5. Adsorbents are not affected by the presence of O_2 if the gas is humidified.

Gray et al. [43], Maroto-Valer et al. [74] and Arenillas et al. [6] prepared several amine-impregnated solid sorbents by chemical treatment of carbon-enriched fly ash concentrates with many amine groups. It was noted that the impregnation of amines caused a drastic decrease in the surface areas, mesopore and micropore volumes of the solid supports. Pore filling and blockage due to the amines were the main cause of these reductions which lead to reduced adsorption capacity. Jadhav et al. [55] impregnated zeolite 13X with MEA and observed an increase in CO_2 adsorption capacity by a factor of 1.6 at 30°C. A higher capacity of modified support at 120°C as compared to unmodified zeolite was also reported. Physisorption may be dominant at 30°C but despite the reduced pore volume and surface area, chemisorption seems to be the significant reason for adsorption of CO_2 at 120°C. Similar results were reported by Fisher et. al [38] who prepared TEPA impregnated β-zeolite and compared it with TEPA-modified silica and alumina. TEPA-impregnated β zeolite due to its high surface area, outperformed the other prepared solid sorbents by exhibiting a continuous capacity of 2.08 mmol g^{-1} at 30°C for over 10 adsorption/desorption cycles.

Overall, literatures show that amine impregnated silica adsorbents exhibit high adsorption capacity, selectivity and kinetics for CO_2 capture at low CO_2 partial pressure conditions. The performance of these adsorbents is reported to be enhanced in the presence of moisture which is very promising owing to the humid nature of the flue gas. However, amine leaching, durability and slow regeneration kinetics of these materials still needs to be adequately researched.

2.2.2 Amine Grafted Adsorbents

Despite the high CO_2 adsorption capacity of amine-impregnated adsorbents, thermal stability during desorption is still a concern that needs to be addressed [20]. As a result, aminosilanes covalently grafted onto the intrachannel surface of the mesoporous silicas through silylation was proposed. The covalent bonding of the amine to the sup-

port improves the thermal stability of the amine and prevents leaching. Many studies have been conducted on amine-grafted silica adsorbents using aminosilanes such as (3-aminopropyl)triethoxysilane (APS), N-[(3-trimethoxysilyl)propyl]ethylenediamine (2N-APS) and N-[(3-trimethoxysilyl)propyl]diethylenetriamine (3N-APS) [112].

First work on amine grafted adsorbents was reported by Leal et. al [67] using APS-grafted silica gel for capture of CO_2 by the formation of ammonium carbamate in dry conditions and ammonium bicarbonate in the presence of moisture. Each of the two amino groups in bicarbonate reacted with CO_2 molecules individually. The overall capacity of the sorbent was observed to be 0.41 mmol/g and 0.89 mmol/g at room temperature in dry and moisture laden atmospheric conditions, respectively. Their adsorption capacity however, is far below the requirement for commercial application of the adsorbent. APS and 3N-APS grafted hexagonal mesoporous silica (HMS) and amorphous silica gel for enhanced CO_2 capture were prepared by Chafee et al. [62], [64], [13], [63]. The grafted HMS sorbents were observed to have a very high surface area with varied extent of surface grafting, influenced by diffusion of amines in pores, surface amount of silanol groups and support porosity. The modified HMS sorbents also displayed a substantially higher CO_2 adsorption capacity as compared to modified silica gel.

Hiyoshi et al. [52], [53] synthesized a series of amine-grafted SBA-15 and studied the effects of the amine natures, pretreatment of support and moisture on CO_2. It was observed that the grafting led to a decrease in the surface area of the amine-grafted SBA-15 but was still higher than the impregnated samples. The group determined that for SBA-15 grafted with APS, 2N-APS and 3N-APS, the CO_2 adsorption capacity in both hydrous and anhydrous conditions the order was:

$$\text{3N-APS} > \text{2N-APS} > \text{APS}$$

But the amine efficiency order was in reverse for the same amine loading due to the presence of 3 amino groups in 3N-APS, 2 in 2N-APS and 1 in APS.

Sayari's group have contributed to design high-capacity, water-tolerant amine grafted silica sorbents with large pore volume and size to facilitate large amine loadings. They performed comprehensive study on amine-grafted MCM-41 and pore-expanded MCM-41 (PE-MCM-41) grafted with amine, such as 3N-APS. It was observed that the pore

size and pore volume influenced the rate of adsorption and adsorption capacity directly. Moreover, Harlick and Sayari [46] revolutionized the conventional grafting (dry solvent with excess of silane) by determining the favourable conditions for grafting 3-[2-(2-aminoethylamino)ethylamino]propyltrimethoxysilane (TRI) on PE-MCM-41. At T=85°C, 0.3ml of water/g of support and 3ml of aminosilane/g of support increased the total amine content, showing a 90% overall improvement. The sorbent showed good stability over 100 cycles and had an average adsorption capacity of 2.28 mmol/g in pure CO_2 at 70°C [93] and 2.65 mmol/g in 5% CO_2/N_2 at 25^{o}C. The dual effect of pore expansion and sorbent grafting technique resulted in significant gains in terms of adsorption capacity and adsorption rate [92].

Jones et al. [29], [51] designed a novel covalently tethered Hyperbranched Aminosilica (HAS) sorbent (Class 3) Figure 2.2 with high amine loading for capturing CO_2 reversibly from flue gas and was compared to other covalently supported adsorbents. The HAS adsorbent developed by a one-step surface polymerization reaction of aziridine monomer inside SBA-15 pores showcased an adsorption capacity of 3.08 mmol/g in a packed-bed reactor in 10% CO_2/Ar hydrous flow at 25^{o}C. Drese et al. [29] improved this work and modified the HAS synthesis conditions, primarily the arizidine-to-silica ratio and the solvent. This resulted in higher adsorption capacity owing to higher amine loadings which directly corresponded to higher potential active adsorption sites.

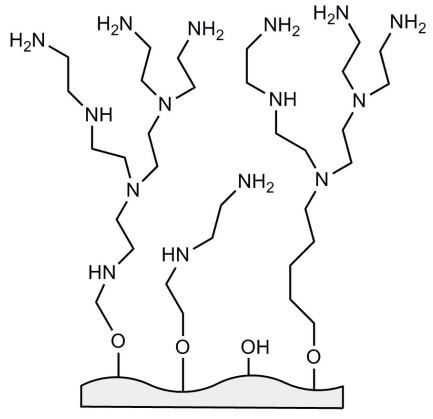

Figure 2.2: Hyperbranched amino silica

In conclusion, amine leaching has been minimized to a large extent by grafting and the thermal stability has been proven without any degradation in the performance of the grafted sorbents [59]. Several of the sorbents tested have theoretical regeneration energies lower than the benchmark of the industry. But lower adsorption capacities and complex synthesis procedure makes grafted amines a less lucrative prospect in comparison to a much simpler impregnation technique. Amine impregnated amines equipped with an optimized regeneration technique capable of countering the amine leaching problem and promising cyclic deployment, will be the best candidates suited for industrial application.

2.3 Regeneration Methods for CO_2 Capture

Once the CO_2 adheres to the surface of the adsorbents and equilibrium is attained, desorption of captured CO_2 takes place to obtain it in pure form. The regenerated adsorbent is then capable of being utilized in the next cycle. This process of regeneration can be performed in different manners, primarily pressure swing adsorption (PSA), vacuum swing adsorption (VSA), vacuum-pressure swing adsorption (VPSA), temperature swing adsorption (TSA), electrically induced thermal swing adsorption (ESA), microwave heating and vacuum thermal swing adsorption (VTSA). For industrial application, an effective and less-energy consuming regeneration method is definitely needed for successful implementation of any adsorbent.

2.3.1 Pressure/Vacuum Swing Adsorption

This technology is widely used in industrial gas separation technologies and is based on reducing the total pressure of the system to carry out the regeneration. In PSA, adsorption is carried out pressures higher than atmospheric, while regeneration is conducted at atmospheric pressure. Conversely, in VSA, adsorption is carried out at atmospheric pressure and desorption is at lower pressures. Both PSA and VSA are based on the principle of difference in adsorption capacity of the adsorbent at higher feed pressure and lower desorption pressure. The difference is termed as working capacity and is shown in Fig 2.3. PSA has been readily applied in a variety of indus-

trial applications such as air separation, air drying, hydrogen purification, methane upgrading, hydrocarbon separation etc.

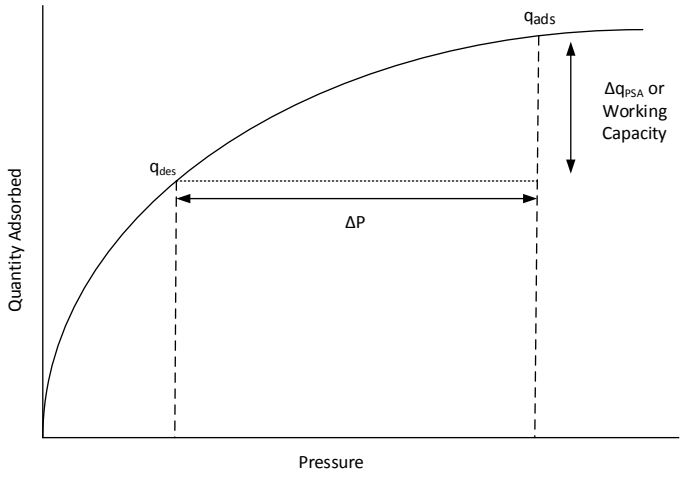

Figure 2.3: PSA Working Capacity

Skarstrom [98] was the first to design a PSA process for separation of a component with high very high purity. This cyle includes two beds packed with the respective adsorbent and is subjected to four steps, namely:

1. Pressurization
2. Adsorption
3. Blowdown
4. Purge or Evacuation

Column 2 is pressurized to the high pressure and column 1 is kept at the low pressure in the first step of adsorption. Next, adsorption takes place in column 2 at high pressure while column 1 is purged at low pressure with the raffinate of the product from high pressure adsorption taking place in column 2. Role reversal takes place over the next two steps in the two columns. Column 1 now repressurized using the

high pressure feed stream followed by high pressure adsorption in step 4 and column 1 is blown down to the low pressure and purged at low pressure.

Generally, the adsorbents used for this technique should have high adsorption capacity, high selectivity towards CO_2 and low regeneration requirements. In PSA, if the heavy component is very strongly adsorbed, high vacuum has to be applied to get a good working capacity, leading to increase in energy required which ultimately increases the operating cost of the process. Therefore, PSA is best suited for materials with linear or slightly non-linear isotherm.

PSA/VSA depict promising scenarios mainly due to the fast regeneration times and overall purity of the adsorbed species, but the technology still has many implications for utilization as CO_2 separation process [48]

1. *Low purity CO_2 recovered:* As discussed briefly above, the process can yield a low recovery for weakly adsorbed species at high purity and conversely yield a high recovery with low purity for strongly adsorbed components. This aspect shows that the process tends to favour the applications in which less strongly adsorbed species is the major product. But in the case of post combustion capture of CO_2, due to its larger electric quadrupolar moment, CO_2 is adsorbed more strongly than the remaining species in flue gas. Heavy-reflux PSA is one of the methods to recover heavy components using PSA. In this process, a rinse step is added after the feed to equilibrate the beds and flush out the N_2 (lightly adsorbed) before recovering the CO_2 (strongly adsorbed) in the Skarstrom cycle. Another method called dual-reflux PSA was also developed with in-depth modeling and experimental demonstrations elaborated in [24], [23], [32]. In this PSA process also, a rinse step to improve the recovery of the CO_2 was integrated but it was reported by Park et al. [80] that this rinsing step drastically increased the power consumption.

2. *Large emissions handling:* Implementation of conventional PSA processes for CO_2 capture in flue gas from large anthropogenic sources is very challenging and too expensive [14]. Technical difficulties mainly concern the pressurization steps in PSA and the handling of the enormous flow of flue gas stack for a standard power station [48].

3. *Variable composition of flue gas:* As shown in Table 1.1 variable flue gas composition are possible depending on the source of emissions. The variations in the levels of impurities like SO_x, NO_x, O_2 and moisture depending on the fuel and combustion type also needs to be considered. As reported [47], VSA is the most cost effective process for CO_2 capture from flue gas where its concentrations is more than 20% at moderate flow rates. The economics for post combustion capture of CO_2 can only be optimized by selecting processes best suited to handle the composition of CO_2 at a manageable flow rate for the given industry.

However, due to the growing interest in these processes there has been a lot of recent developments in terms of research on PSA/VSA. Some of the process optimization and variation studies have been discussed in the following paragraphs.

Smith and Westerberg [99] developed a cyclic operating schedule of a PSA system using mixed-integer nonlinear programming (MINLP) model and simplifying it to a mixed-integer linear programming (MILP) model. The solution of the model predicts the optimal operating configuration (number of beds and their schedule of operations), size and operating conditions which are necessary for determining the minimum annualized cost. Nilchan and Pantelides [78] developed a system of partial differential and algebraic equations to describe the adsorber bed used for PSA in both spatial and temporal domains. A commercial nonlinear programming (NLP) software was employed to solve the large-scale NLP model for use in air separation. They further proposed the use of Rapid PSA and modified PSA processes for air separation without considering the temperature effects. Ko et al. [65], [66] used a method of centered finite differences for the discretization of the spatial domains, and a reduced space sequential quadratic programming (SQP) based approach for the optimization of PSA and fractional vacuum PSA processes for CO_2 capture. They improved the purity of CO_2 to 90% and recovery to 94% by finding optimal values of decision variables with a given power constraint at cyclic steady state. Agarwal et al. [3], [2] designed superstructure-based approach to design and optimize PSA cycles for post combustion CO_2 capture by predicting a number of different PSA operating steps.

Webley and co-workers [14], [115], [108], [114] have done an extensive research in the field of CO_2 capture by adsorption. They predicted the structure of adsorbents at pore level by studying the effect of pore geometry, size and overall adsorbent porosity on the working capacity of the material used in PSA process using optimization methodology. Solid amine adsorbents due to their water tolerant capabilities are readily being considered for PSA process implementation [33], [8]. Ritter et al. [33] researched the use of CARiACT G-10 silica impregnated with PEI for post combustion capture of CO_2 using a PSA process. They performed a thermogravimetric analysis (TGA) to study the behaviour of the material in industrial conditions. They reported the optimum temperature for PSA to be around 80°C for $P_{CO_2} > 10$kPa and 60-70°C for $P_{CO_2} < 10$kPa.

Kikkinides et al. [60] developed a 4-bed 4-step VSA process and improved CO_2 purity and recovery by facilitating the breakthrough of CO_2 from the light end of the adsorber during heavy reflux and then recycling the effluent from this end back to the feed end of the column. Zhang et al [112] studied and compared 6 and 9 step cyclic processes with their VSA process. They reported that the energy requirements and overall capture costs are heavily reliant on the type of adsorbent, process configuration, and process parameters such as initial feed pressure, vacuum pressure, temperature and purge extents. Ho et al [54] compared the capture costs using high-pressure and vacuum desorption steps to that of costs using MEA absorption process and found them to be comparable. They reported that if the selectivity of CO_2-over-N_2 was higher, the purity of the separated CO_2 could be improved and the overall capture costs could be lowered. Delgado et al. [22] evaluated the feasibility of CO_2 capture using activated carbon (AC) in a VSA using theoretical modeling. They reported a high purity (>93%) and high recovery (>90%) for CO_2 capture from a stream containing 13% CO_2 at 40°C and lower power consumption (<0.12 kWh/kgCO_2) as compared to other processes with similar purity levels.

Another hybrid process of PSA and VSA is vacuum pressure swing adsorption (VPSA). A 4-step Skarstorm type VPSA cycle for coal tar pitch based AC beads was designed

by Shen et al. [96]. For a feed containing 15% CO_2 at 202.65 kPa and 303K a purity of 93.7% with 78.3% recovery was obtained. In another theoretical and experimental study [95] the same group used AC beads in a 2-stage VPSA process and reported a power consumption of 723.6 kJ/kg for 95.3% purity and 74.4% recovery of CO_2. Aaron and Tsouris [1] suggested against the use of PSA and VSA as a stand-alone processes for CO_2 capture using standard adsorbents. They proposed the integration of these processes as a pre-step before an absorption-driven process. This adds to the motivation of development of both adsorbents and processes that would couple best and yield small parasitic contributions to the separation of CO_2 from flue gases. PSA/VSA are good choices for their simplicity and fast regeneration times, but for strongly adsorbed CO_2, very low pressure requirements for recovery will pose a threat to already high operation costs and mechanical energy is certainly more costly than heat [87].

2.3.2 Electric Swing Adsorption

Electric Swing Adsorption (ESA) is a variant of TSA process in which the heat is generated *in situ* by passing an electric current through a conductor, i.e., by Joule effect. The role of electrical conductor can be carried out by the adsorbent (direct ESA) or by some ancillary conductor (indirect ESA). The heating rate depends more on the electrical conductivity of the adsorbent material (in case of direct ESA) than the heat capacity of the source and the rate of heat transfer between the source and the adsorbent [85].

The ESA process presents several advantages such as:

1. Due to its simplicity and ease of applicability as compared to conventional TSA systems, the process can be implemented readily with many process configurations suiting the industry and provides similar results [41]. Purge gas flow rates can be controlled independently of the rate of heating and still yield high purity of the recovered species.

2. Due to faster kinetics, this process enables design of efficient heating solutions and smaller sized equipments.

3. Energy for regeneration is delivered with high efficiency directly to the adsorbent. Compared to conventional TSA, larger heating rates can generally be applied.

4. Heat and mass fluxes during desorption step are in the same direction which improves the desorption performance in terms of kinetics for the process mainly due to thermal and gas diffusion effects.

ESA for CO_2 Capture

ESA has garnered a lot of interest and has resulted in a vast amount of research work [27], [71], [113], [19] in removal of volatile organic compounds (VOC's). ESA was first used as an alternative to TSA due to its higher unit productivity while removing VOC's. The success of ESA to purify gas streams has attracted attention to explore its feasibility in capturing CO_2.

An essential feature of any adsorbent to be used in ESA is its electrical conductivity apart from already desired good adsorption capacity. ACs due to their large surface area, micropore volume and electrical conductivity have been mostly studied for ESA applications. But carbonaceous materials have very low CO_2 loadings and selectivity at low partial pressures of CO_2 (case for almost all flue gas emissions). Other potential materials like zeolites though have high adsorption capacities but due to their inability to conduct electricity require external wiring and cannot be used for direct ESA.

ESA for CO_2 separations was fist employed by Burchell and Judkins [10] at Oak Ridge National Laboratory, USA. They used carbon fibre composite molecular sieve (CFCMS) for separation of mixtures containing CO_2 and H_2S. The monolith was subjected to low voltages while being heated to temperatures below 100^oC. It was observed that on application of 4-5 Ampere at a DC voltage of 1V, the adsorbed CO_2 rapidly desorbed. Grande et al. [42] studied the feasibility of using an AC honeycomb monolith in ESA from CO_2 capture from Natural Gas Combined Cycle (NGCC) power plants having low CO_2 content (4.51%) streams. A mathematical model was proposed, validated and employed in simulations by solving partial differential equations using gPROMS software. The developed ESA cycle comprised

of 4 steps: a) Feed or Adsorption, b) Electrification, c) Desorption and d) Purge. Using this configuration in ESA they were able to obtain a recovery of 89.5% with a purity of 16.4%. The low purity of recovered CO_2 was attributed to the adsorption capacity limitations of the adsorbent at the given feed partial pressure. Another simulation based study [41] was performed by the same group to test a hypothetical adsorbent (zeolite 13X/ graphite composite). Mathematical modeling was performed using gPROMS and a six-step ESA cycle was developed obtaining 80% recovery with 80% purity. The new configuration had a partial recycle of CO_2 as a pre-heating technique which enriched the concentration of CO_2 prior to its desorption. Further improvements which involved dividing the purge into two steps allowed to obtain a purity of 89.8% and recovery of 72% with 1.9GJ of energy consumed to capture a tonne of CO_2.

ESA for CO_2 is still in the early stages of research and the technology has certain drawbacks that need to be resolved before using it for large scale applications. The major drawbacks are:

1. AC with its traditional morphologies of granular or powdered form cannot be used in ESA applications as uniform temperature distribution would not be obtained in Joule heating. Non-homogeneity of contact between the particles is the main reason for the non-uniform temperature in the above morphologies.

2. Electrode properties (density, volume, heat capacity and electrical resistance) along with the column details (size, adsorbent material and its packing) are responsible for major energy losses of the electrification step in an ESA process.

2.3.3 Temperature Swing Adsorption

Temperature swing adsorption processes are based on the periodic variation of temperature of the adsorbent due to the difference in the adsorption capacity of the material at different temperatures. The adsorption step takes place at lower temperature and the regeneration of the bed occurs at higher temperature while maintaining almost constant pressure as shown in Figure 2.4 . This process is usually used for

separation of strongly adsorbed species for which variation in pressure for desorption is not enough. TSA processes are used for trace impurity removal from air, gas or air drying, VOC abatement from process gas streams and solvent recovery.

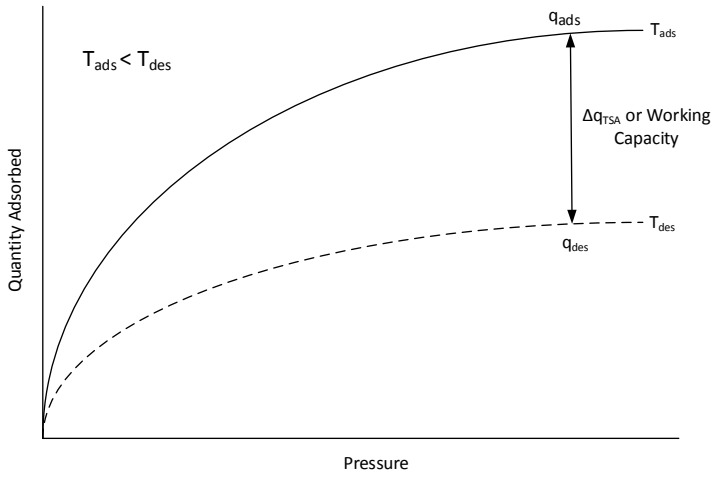

Figure 2.4: TSA working capacity

TSA for CO_2 Capture

TSA process is desired for application in an industrial setting for post combustion CO_2 capture mainly because of the following reasons [106]:

1. Flue gas composition from power plants contain approximately 10% CO_2 which is ideal for TSA process.

2. The adsorbents for TSA must respond to temperature variation in the range of 30^oC-150^oC. This heat can be obtained in a power plant in the form of flue gas waste heat, heat from compression of CO_2, low pressure turbine etc.

3. Since TSA is desired for strongly adsorbed species, thus vastly researched chemisorbents can be employed in this process.

The heat in TSA process can either be provided indirectly or directly using a inert purge gas.

2.3.3.1 TSA by Indirect Heating

An internal heat exchanger is mostly used to heat the adsorbent bed in the regeneration step for this type of TSA process. Merel et al. [75] studied the indirect heating of zeolite 13X for CO_2 removal and reported a 100% recovery of CO_2 while heating the bed indirectly without using any purge gas. The design of their adsorber was heavily influenced from Bonjour et al. [9]. The group later used another way to perform TSA on zeolites 5A and 13X using indirect heating and coupled it with use of purge gas [76]. They passed steam at 150^{o}C in the internal heat exchanger for preheating the sample followed by purging the bed with N_2 once the flow rate of the desorbate was 1.2 Ndm^3/min. The introduction of the purge gas improved the volumetric productivity and specific-heat consumption which in turn reduced the regeneration time as compared to the case with no purge gas. Pirngruber et al. [81] studied and predicted that indirect heating of an amine immobilized solid support would give best results in fixed bed configuration as compared to fluidized bed configuration. They observed that the fixed bed performed better due to the high thermodynamic driving force in the fixed bed. Clausse et al. [18] performed experimental and numerical parametric studies on zeolites 13X and 5A via indirect heating (internal heat exchanger). They reported that the operating conditions of $T_{des} = 160°C$ with a purge at 0.3 Ndm^3/min would help achieve a CO_2 purity of 95% with 80% recovery while having a specific energy consumption of 3.23 GJ/tonne. They concluded that the TSA process with indirect heating was comparable to other adsorption processes.

2.3.3.2 TSA by Direct Heating

In this process the adsorbent bed gets heated up due to the direct heat transfer occurring between the bed and the inert purge gas (He, N_2 or steam) to desorb the adsorbate. Removal of CO_2 using steam would be discussed separately in this section to highlight the focus of this study.

2.3.3.2.1 a) Direct Heating with Hot Inert Gas

The most typical TSA processes are performed using hot N_2 (inert) purge gas to heat the adsorbent bed which facilitates the thermal and concentration swing for removal of adsorbate (CO_2 in case of post combustion capture). Due to the easy handling and safe use of the inert gas in a lab environment, this is the most extensively used method for testing the performance and applicability of new sorbents for CO_2 capture. But the low purity of the species of interest and difficult separation of the inert gas from the desired product makes this process inefficient.

Amine based sorbents can become unstable when exposed to high temperatures under dry inert gas atmospheres. For this reason Zhao et al. [116] studied the thermal stability of TEPA and PEI under N_2 under optimal temperatures used for TSA for such materials. They observed that TEPA started evaporating from the silica support at 100°C and at around 200°C the silica started losing the amine at a rate of 2.2 wt%/min. PEI based adsorbents were observed to be quite stable at temperatures below 150^oC and showed no weight loss. Stripping in the presence of pure CO_2 stream at temperatures of 130°C-180°C was studied by Drage et al. [28]. They observed that at temperatures above 135°C the adsorption capacity of the PEI loaded sorbent reduced drastically. This was attributed to the bonding of CO_2 into the PEI polymer and leading to the formation of stable urea linkages which ultimately lead to the irreversible degradation of the adsorbent. Based on their observations, the group suggested the use of steam as a stripping agent to facilitate the regeneration of the adsorbent and overcome the degradation issues observed in the case of CO_2 stripping.

2.3.3.2.2 b) Direct Heating With Steam

Steam stripping for CO_2 capture has been recently suggested strongly [28], [70], [88]. Regeneration using this process is a feasible method because of the easy availability of low temperature steam in plants as waste heat without any additional costs. Also, unlike inert gases, steam would provide a thermal driving force in addition to the concentration swing for desorption of adsorbed CO_2; thus, improving the kinetics of

the overall process. The most crucial aspect of this technology is that the moisture in the product stream can be easily condensed out unlike inert gases and a concentrated CO_2 product stream can be further compressed and sent for storage or utilization. Though steam stripping is commonly used in MEA absorption process but there are very limited studies conducted to determine its applicability on CO_2 capture using solid adsorbents. Dutcher et al. [30] were the first to explore the impact of direct steam heating on desorption of CO_2. The group also wanted to see if the carbon filter process was feasible when steam was used in conjugation with VSA. They observed that the desorption using steam was rapid producing sharp transition to CO_2, but the steam condensed onto the surface and in the voids of the particles. The accumulation of water over the cycles had a detrimental impact on the adsorption capacity of the sorbent as it decreased by 1 wt% (from 1.7 wt% to 0.7 wt%) in a span of 4 cycles. Water-free VSA carried out at vacuum below 30 Torr produced more than 95% pure stream of CO_2 but the energy consumption was considered to be significantly large. Steam assisted VSA process was proposed to prevent the condensation of steam and at the same time lower the vacuum requirement in VSA. In another study [31], the group performed the earlier proposed study in which VSA was used for desoprtion initially but as soon as a vacuum below 30 Torr was achieved, steam was used to maintain this pressure. They were able to recover 98% CO_2 with 98% purity for over 100 cycles. The energy consumption for the process was deemed infeasible mainly because of the low adsorption capacity and selectivity of the AC towards CO_2 in the presence of moisture. Amine based adsorbents display high selectivity and adsorption capacity for CO_2 and their ability to perform in steam environment is discussed further.

Jones group has been a pioneer in CO_2 capture and have also researched into stability of amine based sorbents [70], [15], [69] in the presence of steam. The group studied the effect of exposure to steam (160°C-180°C)for 24h on the stability of amine and solid support using mesocellular foam (MCF) functionalized using HAS (silica polymerized with Aziridine), PEI, Mono (APTMS) and DMA (AEAPTMS). They observed that the support suffered significant loss in porosity and surface area due to exposure to steam. The CO_2 adsorption capacity was reduced in all cases mainly due to

a)structural collapse of the thin-walled MCF and b)amine degradation due to exposure to steam at high temperature for a long duration. They reported the stability trend to be as:

$$\text{MCF-HAS} > \text{MCF-PEI} > \text{MCF-Mono} > \text{MCF-DMA}$$

The same group also developed PEI impregnated γ-alumina samples possessing large mesopores, large pore volume and basicity. These adsorbents were tested in steam environment for CO_2 adsorption capacity, amine efficiency and stability in comparison to silica impregnated adsorbents [15]. The PEI impregnated mesoporous γ-alumina outperformed the impregnated silica adsorbents in all areas even after suffering a decrease in adsorption capacity of 16.3% as compared to 67.1% for silica based adsorbents.

Gray's group has contributed in studying amine interaction with steam in an immobilized system [107], [34], [45] undergoing cyclic processes. They first studied silica impregnated in a mixture of PEI and APTES and observed a decline of 14% in the adsorption capacity when exposed to moisture (8% in feed). They concluded the polymeric compound was washed away from the pores of the amine and thus reducing the adsorption capacity of the adsorbents. In another study by Hammache et al. [45] a multi-cycle steam regeneration process was developed for PEI impregnated silica in a packed bed reactor. Contrary to Jones and Gray group, they observed the impregnated silica to be unaffected in steam environment. The observed decrease in adsorption capacity was attributed to the re-agglomeration of amine which resulted in an overall reduction in the total number of sites available for CO_2 adsorption. To determine a rapid method of testing a sorbent for use in Basic Immobilized amine sorbents (BIAS) for CO_2 capture Wilfong et al. [107] developed a method of contacting liquid water with sorbent for 40 mins and further exposing it to steam for 10h. They observed that the adsorption capacity was reduced by 73% in the worst case and attributed leaching, evaporation of the active amine sites and amine rearrangements inside the pores as the most likely factors affecting the adsorption capacity. In a recent study performed in our group, Navjot et al. [90] performed regeneration of PEI

impregnated solid sorbent using steam. They reported the sorbent to be highly stable under steam environment with no changes in amine loading, surface morphology and amine linkages even after 5 hours of continuous exposure of the sorbent to steam. The improved performance and adsorption capacity of the sorbent when exposed to humid flue gas along with higher purity of the strongly adsorbed species in the case of steam stripping as compared to N_2 was also reported.

Overall, it can be concluded that there is a significant scope of improvement in the application of solid adsorbents for CO_2 capture. The methods of steam stripping for solid adsorbent regeneration are still in the preliminary phases of research and the process needs to be further improved to maximise the purity and recovery of CO_2 while having short cycle times and competitive energy consumption as compared to current solutions. The easy availability of low pressure steam in power plants as waste heat and especially in coal-fired power plants; along with simple separation of steam and CO_2 by condensation makes this process lucrative and feasible.

Chapter 3

Experiment and Analysis

3.1 Introduction

Silica impregnated with PEI synthesized by the previous researchers in Prof. Gupta's group was used for this study. The material was studied after synthesis using characterization methods of N_2 adsorption/desorption, SEM, CHNS analysis and FTIR analysis and the results of these can be found elsewhere [90]. The synthesized sorbent was used to obtain the equilibrium adsorption isotherms of pure CO_2 for a range of pressures from 0.15 bar upto 1 bar. The isotherms were measured by varying the partial pressure of CO_2 at temperatures of 348.15K, 363.15K and 378.15K. This chapter provides the description of the TGA experimental set-up and functioning methodology used to evaluate the performance of the amine impregnated sorbent samples. Apart from the method used, the analysis of the collected results and derivation of appropriate equilibrium isotherm parameters will also be discussed.

3.2 Experimental

3.2.1 Materials

Commercial grade silica (grade Q-10) from Fuji Silysia Chemical Ltd. was used as a solid support for the amine based adsorbent. The physical material properties of the silica as provided by the manufacturer are: particle density of 1275 kg/m^3 and par-

ticle size distribution of 75-150 μm. For amine impregnation, 99.9% pure methanol from Fisher Chemical and branched PEI having M_w ~800 from Sigma Aldrich were used as obtained. For adsorption measurements, pure CO_2 (99.99%), ultra pure N_2 (99.999%) and a calibrated CO_2-N_2 mixture (1:9 vol/vol) gas cylinders were obtained from Praxair.

3.2.1.1 Adsorbent Synthesis

The amine functionalized adsorbent was prepared by Sandhu [90] using wet impregnation technique [110] as mentioned in detail elsewhere [90]. Detailed schematic outlining the mechanism of amine impregnation has been shown in Figure 3.1. Silica impregnated with 40 wt% PEI was used for this study.

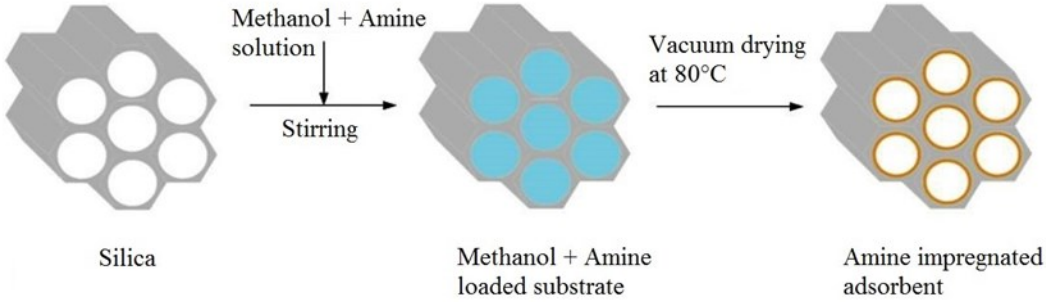

Figure 3.1: Schematic description of amine impregnation mechanism on silica support [116]

3.2.2 Setup and Experimental Procedure

The CO_2 adsorption capacity measurements were obtained using Thermo-Gravimetric Analyzer (TGA/DSC TA Instruments Q600 SDT). TGA was used to obtain an accurate measurement of weight change with respect to the change in temperature. The TGA consists of a horizontal dual beam balance which is used to hold the sample pans. A very thin layer of the adsorbent sample (5 - 10 mg) was placed in a platinum plan along with a reference pan. Through the horizontal purge gas system the sample was heated in N_2 atmosphere at 105°C for 30 min to remove any moisture and CO_2

adsorbed from the atmosphere. The in built digital mass flow control capabilities allow for precise metering of the purge gas that is allowed to flow through the chamber housing the sample and reference pans. After the weight change reached a plateau, the temperature was then decreased to the desired adsorption temperature (75°C, 90°C and 105°C) and the adsorption studies were carried out by varying the partial pressure of CO_2 present inside the chamber. To achieve partial pressures lower than 0.1 bar, the CO_2-N_2 (1 : 9vol/vol) gas mixture was sent into the TGA using the extra gas inlet (reactive port).

Knowing the mass of the adsorbent used for the measurement m_{ads}, the adsorbent capacity can be calculated using the following equations:

$$m_{dry} = m_{ads} \times \text{Lower Point} \tag{3.1}$$

where, m_{dry} is the weight of the sorbent without any moisture or adsorbed CO_2 and Lower Point is the measure of weight% before CO_2 is allowed inside the chamber.

$$m_{adsorbed} = m_{ads} \times \text{Upper Point} \tag{3.2}$$

where, $m_{adsorbed}$ is the weight of the sorbent with CO_2 adsorbed and Upper Point is the point before CO_2 desorption begins.

$$m_{CO_2} = m_{adsorbed} - m_{dry} \tag{3.3}$$

where, m_{CO_2} is the mass of CO_2 adsorbed on to the adsorbent.

$$q = \frac{\text{moles of } CO_2 \text{ adsorbed}}{m_{dry}} \tag{3.4}$$

where, q is in mmoles/g.

3.3 Analysis of Equilibrium Adsorption Data

3.3.1 Single-site Langmuir isotherm

An integral component of an adsorption simulation study is the mathematical modeling of adsorption isotherms in order to gain insight about the behaviour of the adsorbent material. Many widely used isotherms have been described using empirical and theoretical expressions elsewhere [26]. One of the simplest and most commonly used isotherm for describing adsorption equilibria is the Langmuir isotherm. The Langmuir theory is based on the kinetic principle according to which the rate of adsorption is equal to the rate of desorption [98]. Some of the key assumptions of the Langmuir isotherm are:

- All the sites have equal adsorption energies and thus the surface is energetically homogeneous.
- Only one molecule can be accommodated on each site of the sorbent.
- There is negligible interaction between the adsorbed molecules/atoms.

The Langmuir isotherm can be expressed as:

$$q_i^* = \frac{q_{s,i} b_i P_i}{1 + b_i P_i} \tag{3.5}$$

where, q_i^* is the equilibrium solid phase concentration at a given temperature and pressure, $q_{s,i}$ is the saturation solid phase concentration of the given component i and b_i is the affinity parameter. b_i follows the Arrhenius type temperature dependence and relates the adsorption capacity to the temperature by:

$$b_i = b_{0,i} e^{-\Delta H_i / RT} \tag{3.6}$$

where, $b_{0,i}$ is the pre-exponential factor while ΔH_i is the heat of adsorption and T is the temperature at which adsorption is being carried (K). Single-Site Langmuir (SSL) isotherm model has three parameters, $b_{0,i}$, ΔH_i and $q_{s,i}$ which need to be fitted in order to draw any meaningful conclusion from the experimental data. To obtain the unknown parameters, nonlinear regression of the experimental equilibrium isotherm data gathered at different temperatures was performed using the process as shown in

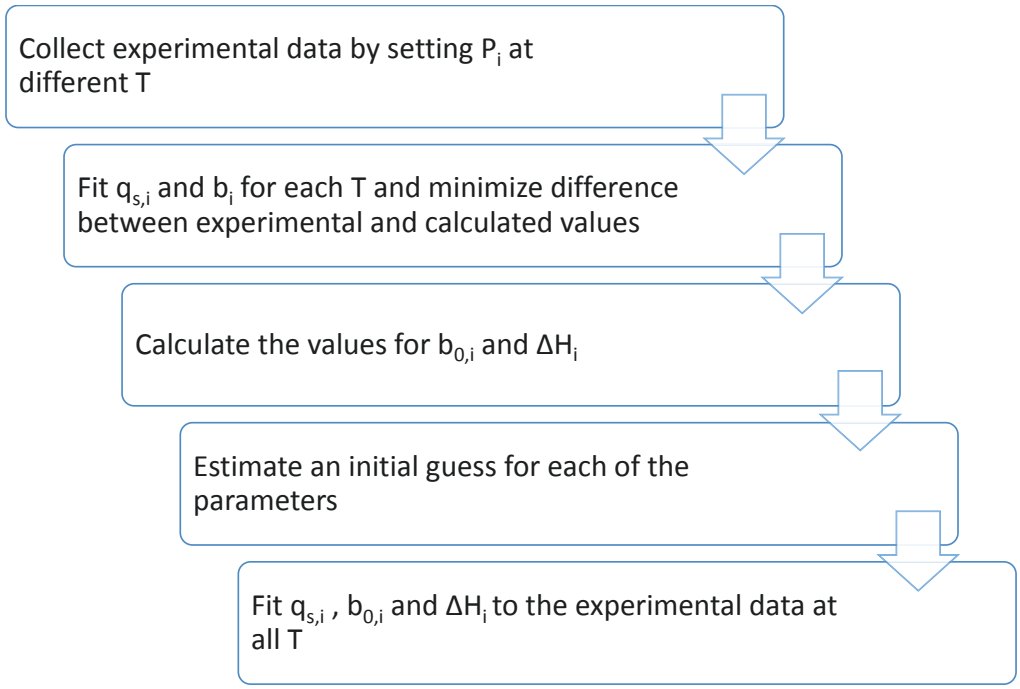

Figure 3.2: Stepwise methodology to obtain single-site Langmuir parameters

Figure 3.2. After getting an initial guess for each parameter, error minimization is done to reduce the error between the experimental and derived values. This gives a sense of the accuracy of the fit while maintaining the integrity of the physical meaning of values for each of the parameters.

3.3.2 Heat of Adsorption

Heat of adsoprtion is the energy released when an adsorbate molecules binds to the adsorbent sites. Since adsorption is exothermic in nature, the heat of adsorption also helps to gain an insight into the expected temperature variations between the different steps of adsorption/desorption cycle, assuming adiabatic process conditions prevail.

There are two ways of expressing the heat of adsorption. There is the integral heat of adsorption, which is the heat change accompanying the isothermal adsorption of a specified quantity of gas or vapour on a gas- or vapour-free adsorbent and the second is the differential heat of adsorption, which is the heat given off when one mole of a gas or vapour is adsorbed by a large quantity of adsorbent already laden with a specified amount of gas [12].

3.3.2.1 Derivation of Clausius-Clapeyron and Van't Hoff equations

The isosteric heat of adsorption can be evaluated from the adsorption-equilibrium data by applying the Clausius-Clapeyron Equation to the two-phase system of gas and adsorbed component on the surface:

$$\left(\frac{\delta P}{\delta T}\right)_{\theta} = \frac{-\Delta H_{iso}}{T(V_g - V_a)} \tag{3.7}$$

where, P is the partial pressure of the adsorbing species at absolute temperature T; $-\Delta H_{iso}$ is the isosteric heat of adsorption and V_g and V_a are the volumes per mole of adsorbed component in the gas and on the surface, respectively.

At low pressures, $V_g \gg V_a$ and the latter may be neglected as small, and assuming the remaining volume of gas V_g follows the ideal gas law at low pressures, Equation 3.7 modifies to:

$$\left[\frac{\delta P}{\delta T}\right]_{\theta} = \frac{-\Delta H_{iso} P}{RT^2} \tag{3.8}$$

where, R is the universal gas constant.

Rearranging Equation 3.8, we have:

$$\left[\frac{\delta P}{P}\right]_{\theta} = \frac{-\Delta H_{iso}\delta T}{RT^2} \tag{3.9}$$

For the Clausius-Clapeyron equation to be valid the process must be univariant, therefore assuming that ΔH_{iso} is invariant, Equation 3.9 can be integrated to:

$$\ln P = \frac{-\Delta H_{iso}}{R}\left(\frac{1}{T}\right) + Constant \tag{3.10}$$

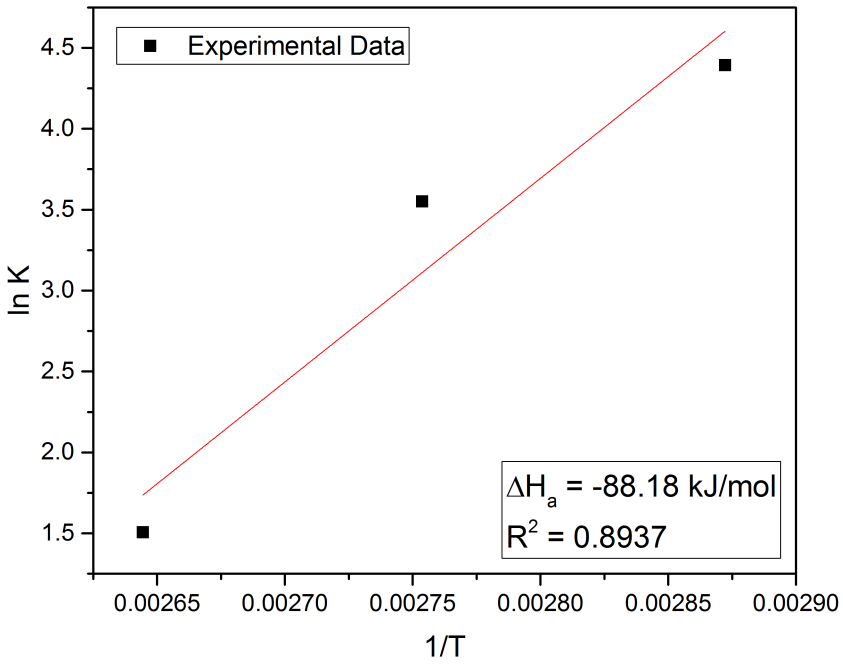

Figure 3.3: Heat of adsorption evaluation using Van't Hoff Equation

This is the Clausius-Clapeyron equation applicable at low pressures.
Similarly, the heat of adsorption can be calculated linearized form of the Henry's equation (Van't Hoff Equation) for the single-site Langmuir model:

$$\ln K = \frac{-\Delta H_a}{R}\left(\frac{1}{T}\right) + Constant \tag{3.11}$$

Using the equilibrium adsorption data for different temperatures, the slope of lnK vs $1/T$ at constant θ can be used as shown in Equation 3.11 to calculate ΔH_a as shown in Figure 3.3. The calculated value of ΔH_a was -88.18 kJ/mol which is in agreement to the values reported in literature for covalently-tethered-silica-supported amines. The values for such adsorbents are distributed in the range of -48 $\sim$ -90 kJ/mol, depending on the analysis technique used [58] [61].

The -ΔH_a obtained using Clausius-Clapeyron equation can be used as an initial estimate for the curve fitting process shown in Figure 3.2. It can then be compared to the heat of adsorption calculated using the curve fitting method to determine

if the estimation of the strength of bond between the adsorbate and adsorbent is plausible or not. It can be possible that the value for heat of adsorption obtained from curve fitting is lower than the experimental data values. This is because the heat of adsorption obtained from the fitting of adsorption equilibrium data over a wide range gives the average value and is thus expected to be lower than the value obtained from the linear data range of the Clausius-Clapeyron equation as shown in Figure 3.5.

3.3.3 Adsorption Performance

CO_2 adsorption capacity of 40wt% PEI loaded silica was determined at different adsorption temperatures and CO_2 partial pressures in a TGA. The effect of partial pressure of CO_2 was studied by changing the CO_2 concentration from 1.5% to 100%. The temperature effect study was performed for three different temperatures of 75^0C, 90^0C and 105^0C. For each of the adsorption studies, the temperature in the chamber was ramped up to 105^0C and held isothermal for 30 min in N_2 atmosphere to get rid of any moisture and adsorbed CO_2 from the ambient air onto the sorbent. As seen in Figure 3.4 the adsorption capacity for simulated flue gas atmosphere (10% CO_2 and 90% N_2) increased with temperature and reached a maximum of 2.31 mmol/g at 75°C. Any further increase in temperature caused the adsorption capacity to decrease. This behaviour has been observed for amine based sorbents and discussed in literature [109] [50] [104] [91] [101] [116]. In these studies it was reported that since the CO_2 adsorption on amino groups is exothermic in nature, thus this trend cannot be explained by thermodynamics alone but rather one needs to consider kinetic effects also. The increase in temperature was proposed to escalate the mobility of the gas which increases the kinetics of CO_2 to regions which were inaccessible at lower temperatures. This increased kinetics thus facilitates the increase of CO_2 adsorption with temperature. Xu et al. [109] proposed a similar explanation for observing the same trend with other PEI-impregnated silicas. They reported that the increase in CO_2 uptake with temperature was due to a singular expansion of PEI aggregates within the pores of the substrate. They observed that at low temperatures, PEI is disposed inside the channels as nanoparticles, and the external active sites of PEI

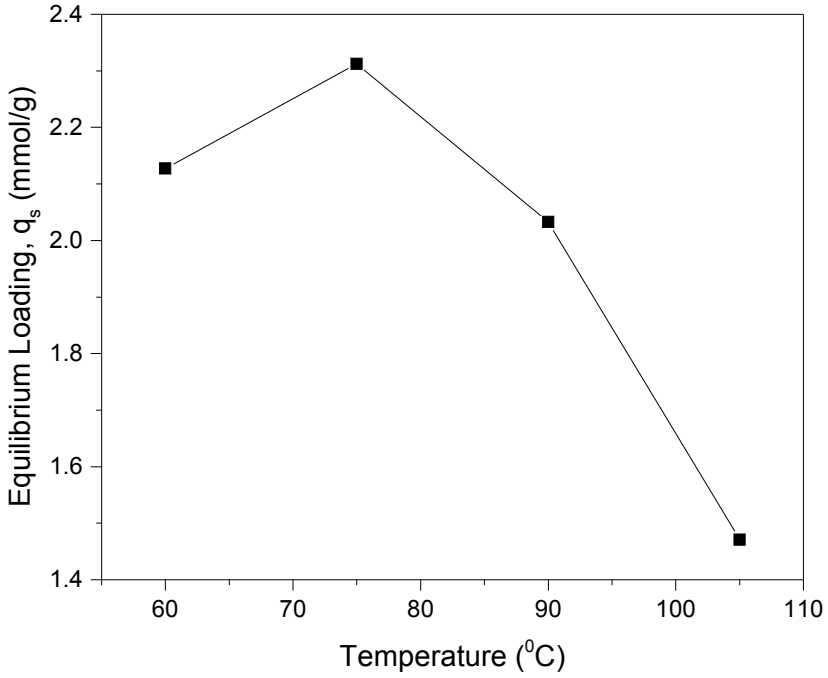

Figure 3.4: Change in adsorption capacity of PEI impregnated silica with increase in temperature at 0.1 bar

on the surface are the ones that can be accessed by CO_2 molecules. Then, as the temperature increases, the PEI expands and is able to occupy all the space available in the pores and thus can be easily accessed by the CO_2 molecules. Since the trend we observed is in close agreement with the theory postulated by Xu et al. [109] and others, we are sure that the synthesized adsorbent is working fine.

To summarize this trend, we can say that the adsorption is kinetically controlled at lower temperatures despite the overall process being diffusion controlled which explains the lower adsorption capacity at lower temperatures. But with the increase in temperature, the diffusional resistances are lowered and at 75°C the diffusional resistances are minimum. After this point, the process becomes thermodynamically controlled and the adsorption capacity decreases with the increase in temperature as expected, deeming the diffusional resistances impotent. This behaviour is consistent with the exothermic nature of adsorption as well. Thus, it can be said that the adsorption on PEI based adsorbents is a balance between kinetic and thermodynamic

forces, with 75°C being the optimum value.

The SSL parameters as obtained from curve fitting shown in Figure 3.5 are:

$$q_s = 2.66 \text{ mol/kg}$$
$$b_0 = 9.42 \times 10^{-12} \text{ bar}^{-1}$$
$$\Delta H = -86.113 \text{ kJ/mol}$$

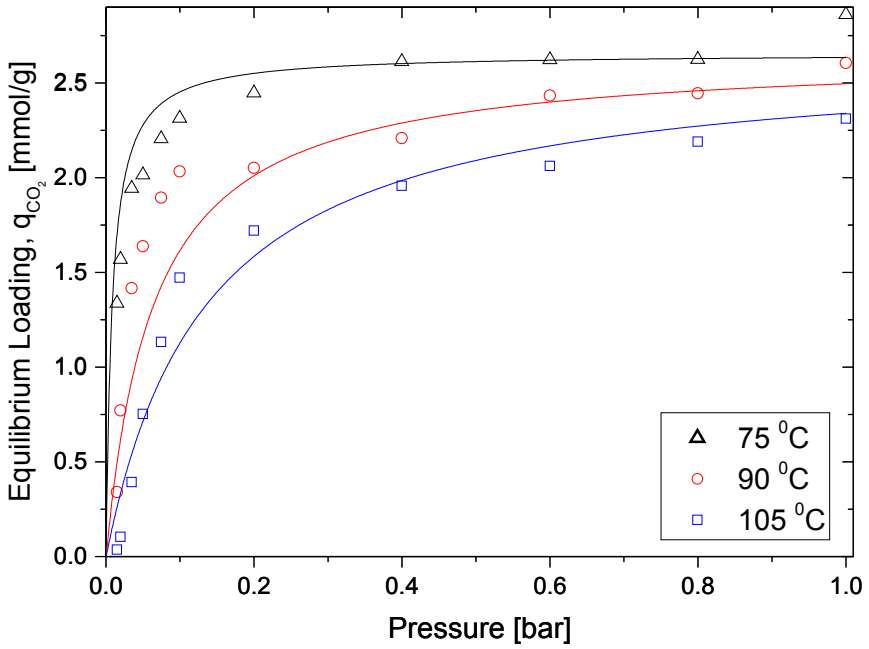

Figure 3.5: Adsorption Isotherm with fitted parameter values. Symbols and lines represent experimental and fitted values respectively

From the single-site Langmuir isotherm in Figure 3.5 it was observed that the maximum saturation capacity of 2.85 mmol/g occurred at 348.15K (75°C). In general, the isotherms for the PEI impregnated silica adsorbent were not very sharp which ruled out the use of low and high pressures being employed to desorb the gas. The results clearly indicated that the adsorbent needs to be operated at 348.15K (75°C) for adsorption and temperatures in excess of 378.15K (105°C) for desorption.

Chapter 4

Modeling and Simulation

4.1 Introduction

In this chapter, the detailed simulation process for modeling of full-cyclic TSA system has been described. In the beginning, the importance of modeling and simulation for engineering processes is explained. Then, the choice of simulator is justified by outlining its capabilities in handling concentration, temperature and pressure dynamics along the adsorption column. The simulator used was tested to accurately predict the behaviour of the designed adsorption system by efficiently incorporating the equilibrium data for the solid adsorbent provided by the user. Further, the model assumptions and momentum, mass and heat transport equations used in the consecutive steps of the process are described. Finally, a validation of the model, based on column dynamics with respect to mass, heat and momentum balances is performed and compared with literature.

4.2 Modeling

4.2.1 Role of Modeling in Engineering Problems

Modeling is used in engineering as a tool to get an estimation of the behaviour of systems and processes. Chemical engineering uses this tool actively and is benefited from it in many ways. Modeling is used to estimate the effectiveness of a unit under

the given conditions and investigate the effect of variation in operating conditions on the product of the systems. But most importantly control and optimization of any system can be achieved with the assistance of modeling to maximize the performance of the process.

4.2.2 Approaches to Modeling and Simulation of Adsorption Processes

Modeling of engineering processes can be broadly classified into two approaches: mathematical modeling and modeling with the aid of process simulators. With the advancement in technology, many processes are now modeled with the aid of process simulators, capable of designing and modeling different chemical engineering units. Some of the well-known simulators which are used by chemical engineers are ProII, HYSYS, gPROMS and Aspen. Aspen is a suite of several packages, each one specializing in different process engineering applications, with Aspen Plus being their flagship software. In this study the adsorption of CO_2 on PEI impregnated silica is studied using process modeling. As the first step, a suitable process simulator which can replicate the operation and predict the behaviour of an actual adsorption unit needs to be selected/designed.

Aspen Adsorption is a package in the Aspen suite which specializes in the simulation of adsorption processes. The software was earlier known as Adsim, which is short for adsorption simulator and was selected as the most suitable process simulator for the purpose of this study. Aspen Adsorption and its various utilities are discussed in the next section.

4.3 Aspen Adsorption

Aspen adsorption is a comprehensive process simulator developed for the optimal design, simulation, optimization and analysis of adsorption processes. Aspen adsorption is widely used in the industry by engineers and end users to optimize and simulate a wide range of gas and liquid adsorption processes. The software can be readily used

to design better adsorption cycles, improve general plant operations and also screen and test potential adsorbents. Some of the features and advantages of the software are outlined in the next few sections.

4.3.1 Features

Aspen adsorption is capable of handling and simulating both small scale laboratory/pilot plant and industrial scale processes. The software can be used to model PSA, TSA, VSA and other variants of these with a wide range of solid adsorbents such as molecular sieves, silica gel, alumina, zeolites and activated carbons. In addition, various separation strategies taking into considerations such as single and multi-layers, equilibrium and rate-based mass transfer and cyclic operations. A rigorous adsorbent bed model having different geometries such as vertical, horizontal and radial bed extended in 1-D and 2-D can also be modeled using this software. Axial dispersion in the bed can be studied and included in the material balance. A wide range of kinetic models such as lumped resistance, micro/macro pore and general rate model are built in the simulator. Additionally many standard equilibrium isotherm models such as Langmuir, Freundlich, Toth, Sips and B.E.T. in addition to ideal adsorded solution theory (IAST) are present in the software which allows for either pure component or multi-component competitive behaviour. The software has a highly configurable energy balance which allows the user to simulate non-isothermal behaviour, conduction (solid/gas), non-adiabatic operation and other wall effects.

Besides accurately specifying the adsorbent bed model, Aspen Adsorprion also features the use of steady state and dynamic estimation and optimization techniques for rapid design and optimization of cycles. The software is also capable of parameter regression and can fit model against experimental or process data and regress against steady or dynamic state experimental data.

4.3.2 Benefits

Aspen Adsorption can be used for adsorption process design and can help in reduction of time and costs of laboratory and pilot plant trials which are the major benefit of simulation works. Having a validated model results enables the engineers to understand the process in less time and at the same time protects the crew from potential safety issues and challenges of the real process. As it happens ever so often that a design goes through many alterations before finalizing to a final design, in regards to this, the software gives the user the freedom to configure the process to improve the plant operations in order to determine the effect of various variables on plant performance.

4.4 Model Equations

In order to develop a mathematical model for a one-dimensional dynamic column, the following assumptions were made:

- The gas phase follows the ideal gas law.
- The bulk fluid flow is represented using an axially dispersed plug flow model.
- The bed is initially filled with N_2 in thermal equilibrium with the feed temperature.
- The bed operates in non-isothermal and non-adiabatic conditions with gas and solid conduction.
- Radial mass, pressure and heat dispersion are neglected and only axial dispersion occurs.
- The superficial velocity is related to the total pressure gradient according to the Darcy's law.
- The main resistances to mass transfer are combined in a single lumped parameter, where the mass transfer kinetics within the solid phase can be described by the linear driving force (LDF) model.

- Bed voidage and particle size are uniform across the column.
- The single-site Langmuir model with single component isotherm parameters is used.
- Outer column wall is in equilibrium with ambient atmosphere.

Considering the above assumptions, the model equations are as follows.

Ideal Gas Law

$$\mathrm{P}y_i = \mathrm{R}T_g c_i \tag{4.1}$$

Where, P is the total pressure, y_i is the mole fraction of component i in the gas phase, T_g is the temperature in bulk gas phase, and c_i is the concentration of solute i in the fluid.

Mass Balance of Sorbate Species

The mass balance in the gas phase takes into account the effect of the axial dispersion, convection term, gas-phase accumulation, and rate of flux to the adsorbent

$$-\varepsilon_b D_{ax}\frac{\partial^2 c_i}{\partial z^2} + \frac{\partial(v_g c_i)}{\partial z} + \varepsilon_t\frac{\partial c_i}{\partial t} + \rho_b\frac{\partial \overline{q}_i}{\partial t} = 0 \tag{4.2}$$

Where, ε_b and ε_t are the interparticle voidage and total bed voidage, respectively, v_g is the gas-phase velocity, z and t are the axial coordinate and time, respectively, ρ_b is the adsorbent density, and $\overline{q}_i$ is the average amount of solute i adsorbed. The dispersion coefficient D_{ax} varies along the length of the bed following the correlation [86].

$$D_{ax} = 0.73D_m + \frac{v_g r_p}{\varepsilon_b\left(1 + 9.49\dfrac{\varepsilon_b D_m}{2v_g r_p}\right)} \tag{4.3}$$

Here, r_p is the particle radius. The molecular diffusion coefficient D_m is estimated from the Chapman-Enskog equation.

The boundary conditions for fluid flow are

$$D_{ax}\frac{\partial c_i}{\partial z}\bigg|_{z=0} = -v_g\big|_{z=0}(c_i\big|_{z=0^-} - c_i\big|_{z=0}) \tag{4.4a}$$

$$\left.\frac{\partial c_i}{\partial z}\right|_{z=L} = 0 \tag{4.4b}$$

Momentum Balance

The superficial velocity is related to the total pressure gradient according to Darcy's law

$$-\frac{\partial P}{\partial z} = K_p v_g \tag{4.5a}$$

where P is the total pressure expressed in bars, v_g is the gas phase velocity and K_p is the Darcy's proportionality constant given by:

$$K_p = \frac{150\mu}{4{r_p}^2}\left(\frac{1-\varepsilon}{\varepsilon}\right)^2 \tag{4.5b}$$

Where, r_p is the radius of the solid particles, ε is the bed voidage and μ is the fluid viscosity coefficient calculated using the Chapman-Enskog equation and is assumed to be independent of temperature.

Mass-Transfer Rate

The mass transfer from the gas to the solid phase is expressed by a linear driving force (LDF) model

$$\frac{\partial \overline{q}_i}{\partial t} = k_{MTC_i}(q_i^* - \overline{q}_i) \tag{4.6}$$

where q_i^* is the loading, which is in equilibrium with the gas-phase composition. The effective mass-transfer coefficient, k_{MTC}, is given as a lumped parameter term comprising of the external film resistance and macropore diffusion terms.

Gas-Phase Energy Balance

The gas-phase energy balance includes axial thermal conduction, convection of energy, accumulation of heat, gas-solid heat transfer, and gas-wall heat transfer. The governing partial differential equation is as follows:

$$-\varepsilon_b k_{gz}\frac{\partial^2 T_g}{\partial z^2} + v_g C_{vg}\rho_b\frac{\partial T_g}{\partial t} + \varepsilon_t C_{vg}\rho_b\frac{\partial T_g}{\partial t} h_p a_p(T_g - T_s) + \frac{4h_w}{d_B}(T_g - T_w) = 0 \quad (4.7)$$

Where, C_{vg} is the specific gas-phase heat capacity at constant volume,
a_p = (1-ε_b)3/r_p is the specific particle surface per unit volume of the bed, d_B is the internal bed diameter, and T_g, T_s and T_w are the gas, solid, and internal wall temperatures, respectively.
The boundary conditions for the gas-phase energy balance are:

$$k_{gz}\frac{\partial T}{\partial z}\bigg|_{z=0} = -\rho_g C_{pg} v_g\big|_{z=0}(T\big|_{z=0^-} - T\big|_{z=0}) \quad (4.8a)$$

$$\frac{\partial T}{\partial z}\bigg|_{z=L} = 0 \quad (4.8b)$$

Solid-Phase Energy Balance

The solid-phase energy balance includes axial thermal conductivity, enthalpy accumulation, heat of adsorption, and gas-solid heat transfer

$$-k_{sz}\frac{\partial^2 T_s}{\partial z^2} + c_{ps}\rho_b\frac{\partial T_s}{\partial t} + \rho_b\sum_{i=1}^{n}\left(\Delta H_i\frac{\partial \overline{q}_i}{\partial z}\right) - h_p a_p(T_g - T_s) = 0 \quad (4.9)$$

where k_{sz} is the effective axial solid-phase thermal conductivity and C_{ps} is the specific heat capacity of the adsorbent. The heat of adsorption of component i, ΔH_i, is provided as shown in the previous chapter, page 49.

Wall Energy Balance

The effects considered for the wall energy balance include axial thermal conductivity along the wall, heat content of the wall, and both the gas-wall and wall-oven heat exchanges

$$-k_{wz}\frac{\partial^2 T_w}{\partial z^2} + C_{pw}\rho_w\frac{\partial T_w}{\partial t} - h_w\alpha_w(T_g - T_w) + H_{amb}\alpha'_w(T_w - T_{amb}) = 0 \quad (4.10)$$

where k_{wz} is the thermal conductivity of the column wall, T_{amb} is the ambient atmospheric temperature, C_{pw} are the specific heat capacity and the density of the column

wall, respectively, α_w is the ratio of the internal surface area to the volume of the column wall, α'_w is the ratio of the external surface area to the volume of the column wall and H_{amb} is the wall-ambient heat-transfer coefficient.

Numerical Methods

The set of equations was numerically solved using Aspen Adsorption V8.4. Aspen Adsorption uses the method of lines to solve the time-dependent partial differential equations. The spatial derivatives were discretized over a uniform grid of 20 points by the upwind differencing scheme (UDS1) in conjunction with the Gear integration with a variable step size of 0.1-5 s. The physical properties of the components in the process are locally estimated through integration with the Aspen Properties database.

4.5 Model Validation

To verify the reliability of Aspen Adsorption, a validation study was performed to make sure that the simulator gives a reliable set of data. The validation can be done by comparing the results from the simulator with available experimental work or by performing simulation for work in literature using the simulator. Once the results obtained from modeling for the chosen work are comparable to the results obtained via experiments or some other simulator, the simulation capabilities of the software are deemed reliable and validated.

For testing Aspen Adsorption, case study performed by Haghpanah et al. [44] was used for validation purposes. Haghpanah used a 4-step VSA cycle to demonstrate the working of their schemes. A detailed working of the cycle is shown in Figure 4.1. Step 1 is the pressurization step in which feed containing 15 mol % CO_2 and 85 mol % N_2 at 1 bar and 25°C are fed into the column from the feed end (z=0). The opposite end of the column (z=1) is closed and the system is allowed to be pressurized. In the next step (high pressure adsorption) the feed is continuously fed into the system while the z=1 end is opened for the less adsorbed N_2 to exit and to be collected. Step 3 is the

blowdown in which the feed end is closed and the bed pressures adjusted so as to remove as much as possible N_2 while retaining the CO_2. Final step is the evacuation in which the light product end (z=L) is closed and the feed inlet held open so as to reduce the pressure of the bed which results in collection of high purity CO_2 rich stream.

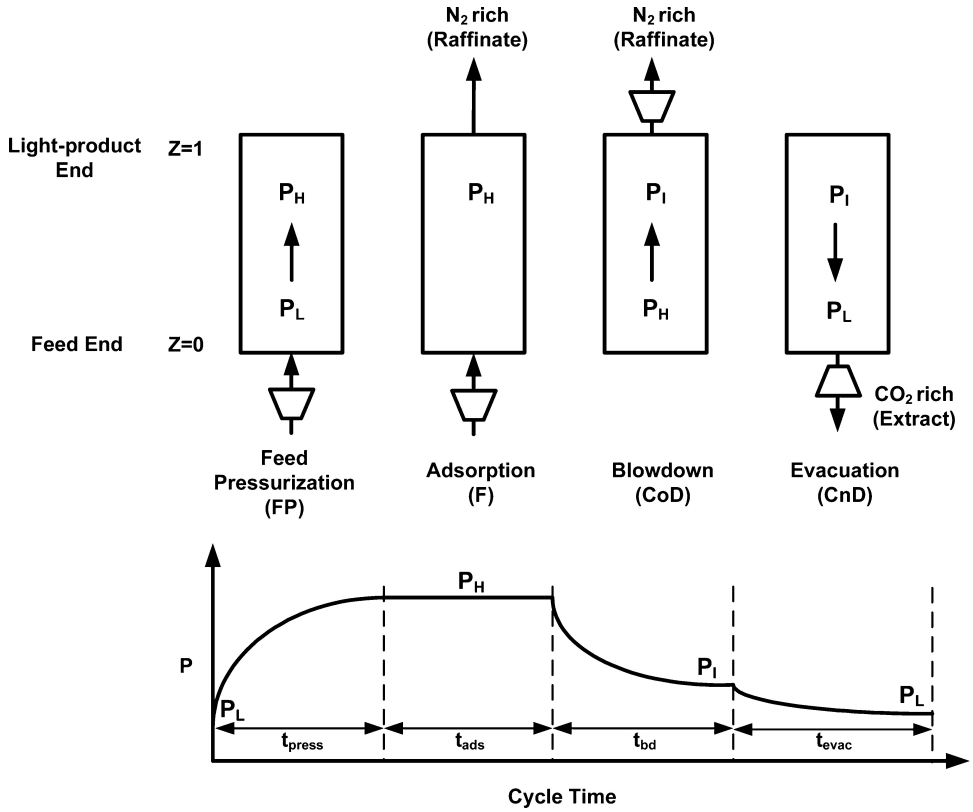

Figure 4.1: 4-step VSA cycle with corresponding pressure profile
Reprinted with permission from Copyright (2013) American Institute of Chemical Engineers

The breakthrough simulations were performed for the parameters mentioned by Haghpanah et al. [44] and using dual-site Langmuir isotherm parameters provided by them. The breakthrough profiles for velocity, temperature and CO_2 for the adsorption step obtained using Aspen Adsorption are shown in Figure 4.2. The results were found to be consistent with the results obtained by Haghpanah et al. and the observed deviations were considered to be in the acceptable range of computational irregularities. Hence, the Aspen Adsorption software was considered suitable for performing further adsorption process studies.

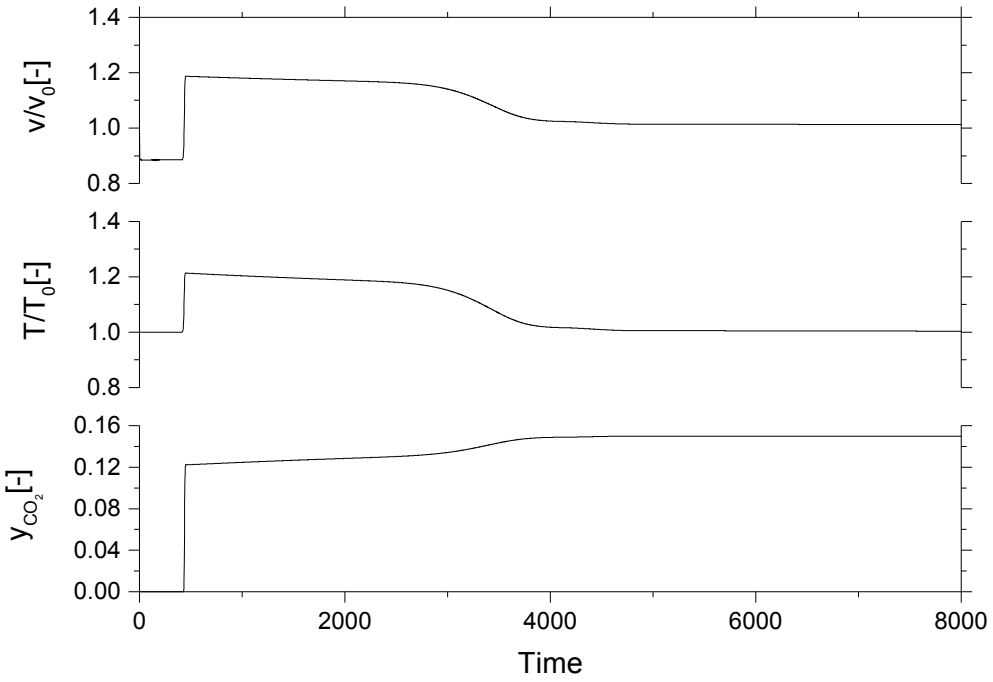

Figure 4.2: Velocity, temperature and composition breakthrough profiles for CO_2 at the exit of the adsorption column. The feed had an interstitial velocity, $v_{feed} = 1m/s$, feed temperature, $T_{feed} = 298.15\ K$ and feed composition of CO_2, $y_{CO_2} = 15\ mol\%$

Once the model was validated, we gained ample confidence in the dynamic modeling capabilities of the software as it was able to predict the adsorption behaviour accurately. As Aspen Adsorption efficiently mapped the mass, momentum and heat transfer effects in conjugation with the validation study, we performed simulations for the specific adsorbent at different process conditions. Also, various cycle configurations to optimize the adsoprtion performance parameters were tested out in order to improve the CO_2 capture process. The development of these topics will be discussed in the next chapter.

Chapter 5

Development of Steam Purge TSA Cycle for Improved Purity and Recovery

5.1 Introduction

In this chapter, the capture of CO_2 from simulated flue gas using two different configurations of TSA processes are presented. Firstly, a basic 3-step cycle is presented and the results are discussed. Then, a new 4-step configuration is developed in order to improve the purity of CO_2 recovered. The boundary conditions for the individual steps in the two TSA cycles are also detailed. The adsorbent and column properties used for the simulation of the two cycles are also tabulated in this chapter. Comparisons between the developed cycles are made in terms of purity and recovery and taking into account the effect of steam purge time step. Further, scaled up models of the bed were developed to see how it affects the purity and recovery.

5.2 Cycle Designs and Configurations

In order to fully utilize the CO_2 capture capabilities of amine based sorbents, it is of prime importance that it should be operated in an optimized cycle configuration. Though there are some cycle configurations mentioned in literature [56] [17], but none of them were found to be convenient for steam regeneration of the amine impregnated

adsorbent. Therefore, we adapted the cycles from PSA so as to study the purity and recovery of CO_2 obtained from these cycles. Purity and recovery have been defined below in Equation 5.1 and Equation 5.2 respectively. For our sorbents, we developed a basic 3-step cycle consisting of an adsorption, heating and cooling steps as shown in Figure 5.1 . A basic overview of the process cycle configuration and the proposed improvements can be found in the subsequent sections.

$$\text{Purity, } Pu[\%] = \frac{\text{Total moles of } CO_2 \text{ in the heating product}}{\text{Total moles of } CO_2 \text{ and } N_2 \text{ in the heating product}} \times 100$$

or

$$Pu[\%] = \left[\frac{mole_{out,CO_2}\big|_{heating}}{mole_{out,CO_2}\big|_{heating} + mole_{out,N_2}\big|_{heating}}\right] \times 100 \tag{5.1}$$

$$\text{Recovery, } Re[\%] = \frac{\text{Total moles of } CO_2 \text{ in the heating product}}{\text{Total moles of } CO_2 \text{ fed into the adsorption step}} \times 100$$

or

$$Re[\%] = \left[\frac{mole_{out,CO_2}\big|_{heating}}{mole_{in,CO_2}\big|_{adsorption}}\right] \times 100 \tag{5.2}$$

5.2.1 3-step TSA cycle

As stated earlier, this cycle consists of three major steps of adsorption, heating (regeneration or evacuation) and cooling. The key features of these steps with respect to the cycle described in Figure 5.1 are explained below:

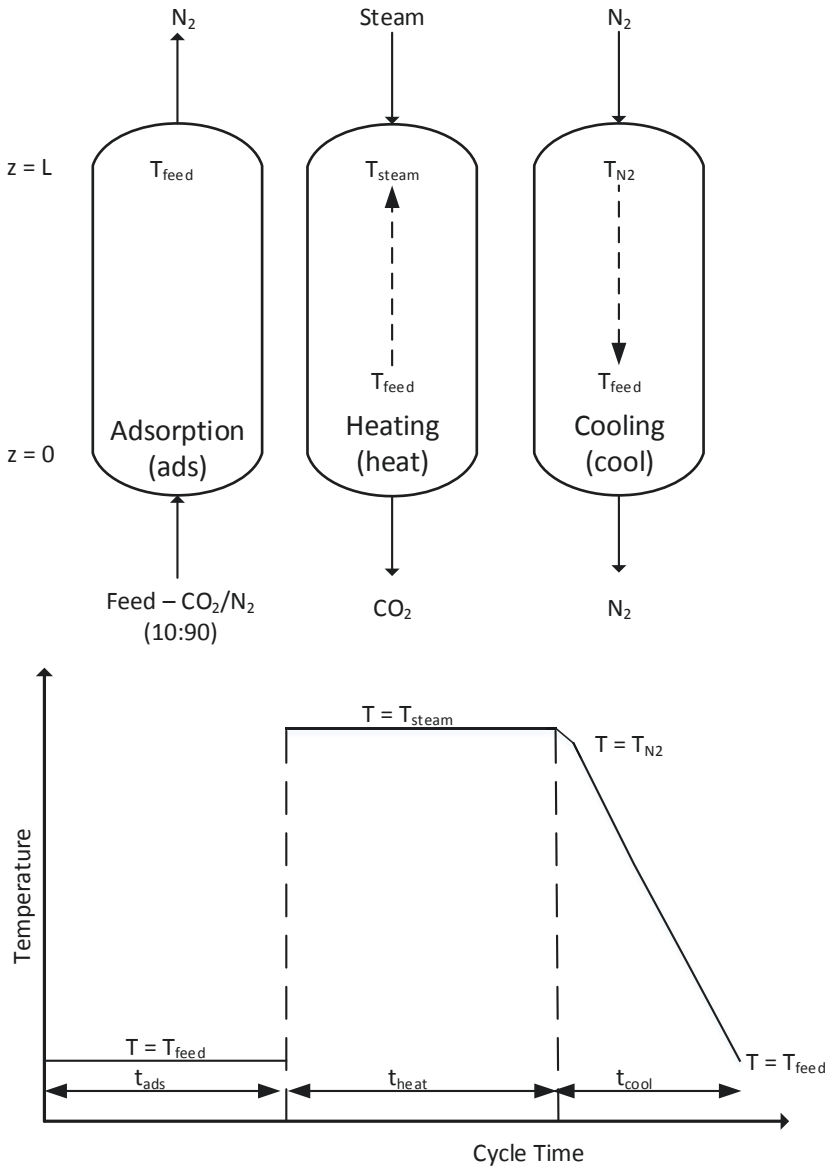

Figure 5.1: 3-step TSA cycle

Adsorption

Prior to the adsorption step, the bed is at atmospheric pressure and at the feed temperature. At this point the bed is saturated with N_2 and there are no traces of CO_2 in either the gas or the adsorbed phase. Flue gas (10% CO_2 and 90% CO_2) is fed into the bed at z=0 end at feed pressure (P_{feed}) and temperature (T_{feed}). In this step, the strongly adsorbing species (CO_2 in this case) binds preferentially to the adsorbent as compared to the weakly adsorbing component (N_2). The top end of the bed, z=L is held open and N_2 is collected from this end. As the bed gets saturated with the feed it is closely monitored so as to prevent any CO_2 loss at z=L end. This prevention of loss of CO_2 in this step is done by keeping the time interval for the step less than the breakthrough time of CO_2 which helps to maximise the overall recovery of CO_2 at the end of the cycle. Due to the exothermic nature of adsorption processes, the temperature of the bed is bound to increase as CO_2 is adsorbed. This increase in temperature lowers the equilibrium loading well beyond the ideal loading observed in an isothermal process. Once the thermal wave travels across the column, the loading would increase further.

Partial differentiation equations for mass and energy balances are solved simultaneously in order to design the complete process and determine the equilibrium loading, breakthrough temperature and time, and the amount of feed required for saturation.

Heating

Since CO_2 is adsorbed in the bed, it needs to be removed so that the bed is prepared for the next cycle. Regeneration of the adsorbent can be done using a pressure or temperature swing process. Here we exploit the difference in the sloid phase loadings by doing a temperature swing with steam. The temperature of the bed is increased with the aid of steam at $403K$ which comes in direct contact with the adsorbent. Special cautions were taken so as to never allow the temperature of the bed to increase above 135°C which could possibly cause the amine to denature and form urea as mentioned in [28]. Since the steam is introduced from z=L end in counter-current manner, the node at the product end of the bed (z=L) would get heated faster than the feed end (z=0). The time interval for this step was kept such that the first node at z=0 end should be higher than 100°C. Due to the increase in temperature of the

sorbent, the CO_2 is transferred from the solid phase into the fluid phase and travels along with steam to be collected at the z=0 end.

Cooling

The final step in this cycle is a cooling purge step using N_2 at 105°C which is linearly cooled down to 75°C at the rate of 10°C/min. Since the bed was saturated with steam at the end of the last step, N_2 fed from z=L end, has to be introduced at a higher temperature than 100°C so as to prevent any steam from condensing in the bed. The N_2 purge serves two purposes, first is to cool down the bed to T_{feed} which would prepare it for the next cycle and second is to remove the residual steam stored in the bed. Though it has been demonstrated that in certain TSA processes a purge cooling step is redundant and the thermal wave in the feed step travels faster than the concentration wave and thus cools the bed during feed itself before the adsorption even takes place [7]. But on further investigation, it can be noticed that due to the lower equilibrium loading, more concentrated feed and higher temperature difference, the flue gas (feed) would be unable to cool the bed unlike many industrial drying processes.

As mentioned earlier, the only CO_2 loss in the cycle could be during the adsorption step if the CO_2 breakthrough occurs and trickles out from the z=L end. The state of the bed at the end of each step is taken as the initial condition for the subsequent step. The column at the end of cooling step should be in the same state as the initial condition for the following adsorption step.

5.2.1.1 Boundary Conditions and Model Parameters

The model equations mentioned in the previous chapter, the initial and boundary conditions must be defined. The boundary condition define the physical and mathematical specifications for each end of the column and are required to solve the differential equations for each of the steps. For the three steps described above, the boundary conditions are summarized in Table 5.1. The parameters for the simulation can be found in Table 5.2.

Table 5.1: Boundary conditions for the various configurations of steps used

	Feed end [z=0]	**Product end [z=L]**
	$D_L \frac{\partial(y_i)}{\partial z}\big\vert_{z=0} = -v\big\vert_{z=0}(y_{i,\text{feed}} - y_i\big\vert_{z=0})$	$\frac{\partial y_i}{\partial z}\big\vert_{z=L} = 0$
All steps (Open-Open)	$\frac{\partial T}{\partial z}\big\vert_{z=0} = -\varepsilon\rho_{\text{g}}C_{\text{p,g}}v\big\vert_{z=0}(T_{\text{feed}} - T\big\vert_{z=0})$	$\frac{\partial T}{\partial z}\big\vert_{z=L} = 0$
	$T_w\big\vert_{z=0} = T_{\text{feed}}$	$T_w\big\vert_{z=L} = T_{\text{feed}}$
	$v\big\vert_{z=0} = v_{\text{feed}}$	$P\big\vert_{z=L} = P_{\text{feed}}$

Table 5.2: Simulation parameters used in TSA cycle modeling

Parameter	**Value**
Column Properties	
Column length, L [m]	0.01
Wall Thickness, W_t [m]	1.75×10^{-5}
Internal column diameter, D_{in} [m]	9.52×10^{-3}
Column void fraction, ε_t [-]	0.37
Particle voidage, ε_b [-]	0.35
Particle radius, r_p [m]	1×10^{-3}
Tortuosity, τ_p [-]	3.00
Fluid and Adsorbent Poperties	
Flue gas pressure, P_{feed} [bar]	1.00
Feed temperature, T_{feed} [K]	348.15
Ambient temperature, T_{amb} [K]	298.15
Column wall density, ρ_w [kg m^{-3}]	7800
Adsorbent density, ρ_b [kg m^{-3}]	1275
Specific heat capacity of the fluid phase, $C_{p,g}$ [J mol^{-1}K^{-1}]	30.7
Specific heat capacity of the adsorbed phase, $C_{p,a}$ [J mol^{-1}K^{-1}]	40.5
Specific heat capacity of the adsobent, $C_{p,s}$ [J kg^{-1}K^{-1}]	1800
Specific heat capacity of column wall, $C_{p,w}$ [J kg^{-1}K^{-1}]	502
Fluid viscosity, μ [kg m^{-1}s^{-1}]	1.94×10^{-5}
Molecular diffusivity, D_m [m^{2}s^{-1}]	1.98×10^{-5}
Effective gas thermal conductivity, K_{gz} [J m^{-1}K^{-1}s^{-1}]	0.09
Thermal conductivity of column wall, K_{wz} [J m^{-1}K^{-1}s^{-1}]	16
Thermal conductivity of adsorbent, K_{sz} [J m^{-1}K^{-1}s^{-1}]	0.1
Inside heat transfer coefficient, h_{in} [J m^{-2}K^{-1}s^{-1}]	8.6
Outside heat transfer coefficient, h_{out} [J m^{-2}K^{-1}s^{-1}]	2.5
Universal gas constant, R [m^{3}bar K^{-1}mol^{-1}]	8.314×10^{-5}

Table 5.3: Process conditions (step times and stream temperatures) for the 3-step TSA cycle configuration

	t_{ads} [s]	t_{heat} [s]	t_{cool} [s]	T_{feed} [K]	T_{steam} [K]	T_{N_2} [K]
3-step cycle	50	250	400	348.15	403.15	398.15

5.2.1.2 Results- Basic Cycle

A basic 3-step cycle was designed and a full cycle simulation was performed using the simulation parameters mentioned in Table 5.2 until the process was completed and the column attained the initial conditions at the end of the cycle. Using the modeling techniques, the dynamics of the bed were simulated and detailed gas phase, solid phase and temperature profiles across the column were generated. On carefully studying many profiles, the individual step times were determined for each of the three steps as optimal process conditions with respect to the overall time and efficiency of the column shown in Table 5.3).

As shown in Figure 5.2 the temperature at node 20 (z=L end) and node 10 increases by 35°C during the adsorption step. This increase in temperature substantially decreases the equilibrium loading at this node, though as the bed cools down after the thermal wave passes, the loading at these nodes would increase. This effect is prominently observed for node 1 (z=0 end) as shown in Figure 5.2 and Figure 5.3 that as node temperature decreases, the loading at that node increases. Since the trickling of CO_2 after breakthrough from the column would lower the recovery, our aim would be to keep it at a minimum. This would be discussed further in this section with more details.

The regeneration of the column was performed using steam at 130°C. This temperature is much higher than ideal because we didn't want the steam to prematurely condense before breakthrough which would make the bed wet. Also from the adsorbent isotherm, it would make sense to use a sufficiently high temperature for regeneration since there is significantly lower loading than the feed condition at this temperature.

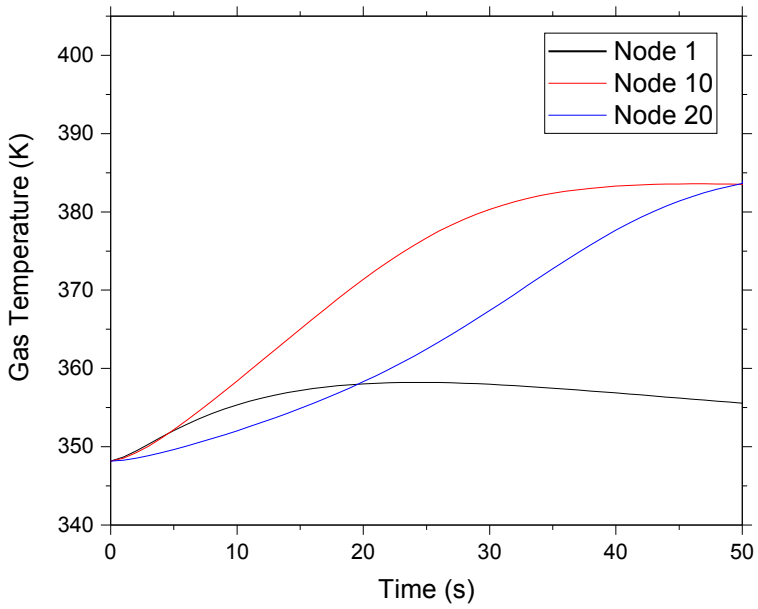

Figure 5.2: Gas temperatures at Node 1, 10 and 20 at the end of adsorption step in a 3-step TSA cycle

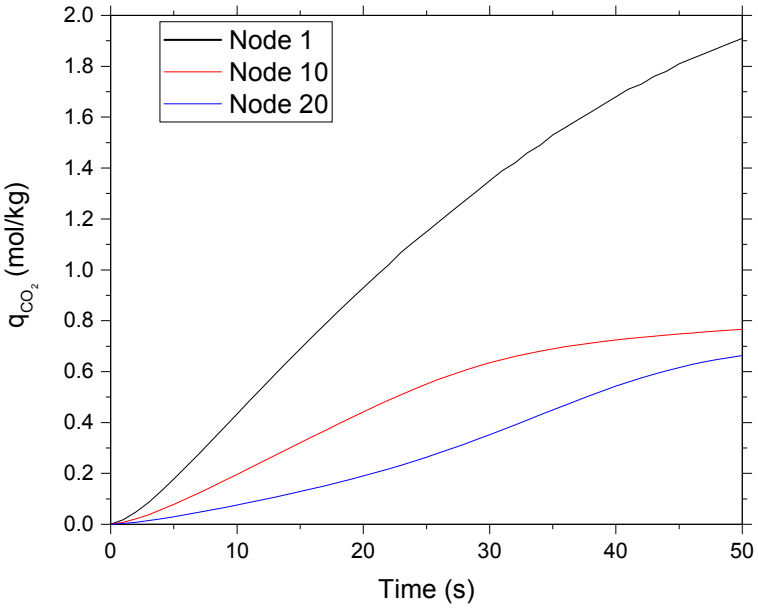

Figure 5.3: Solid loadings at Node 1, 10 and 20 at the end of adsorption step in a 3-step TSA cycle

The steam was successful in heating the bed as seen in Figure 5.4 and stripping the CO_2 off completely which is clearly visible from the solid phase profiles shown in Figure 5.4. Furthermore, it should also be noted that steam will push out the CO_2 and N_2 present in the fluid phase along with the CO_2 contained in the solid phase.

As stated earlier, the bed was cooled using N_2 at 105°C and was linearly brought down to 75°C while forcing out the steam present in the fluid phase at the end of heating step. As seen from Figure 5.4 the gas phase temperature does fall instantly from 130°C to 115°C at Node 20 (z=L end) in the first 6 seconds of the cooling step but this is still higher than the condensation temperature of steam. The steam was observed to completely drain out of the system within the first 7 seconds of this step and thus is not condensed in the bed. The rest of the step is mainly dedicated to cooling the bed and preparing it for next cycle. Though feed gas or pure stream of CO_2 could be used to cool the bed, but it was decided not to be very effective in this regime and was not tried in this study.

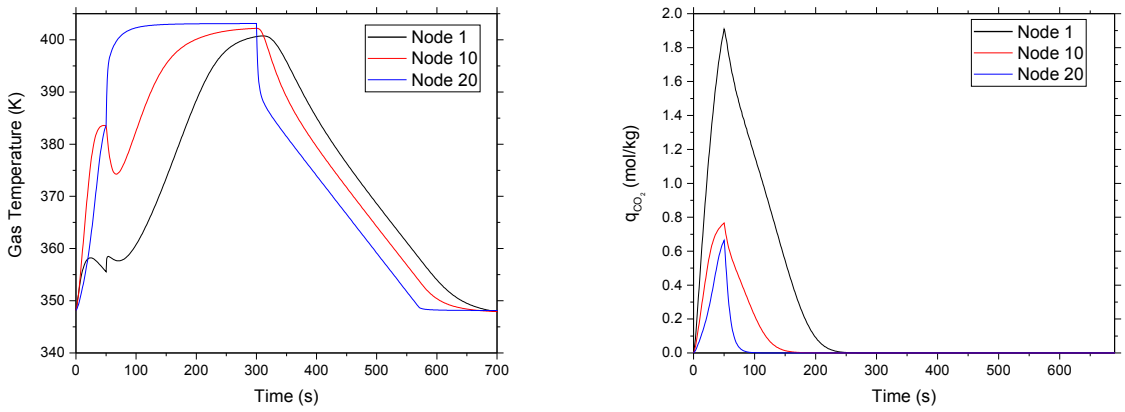

Figure 5.4: Gas temperatures (left) and solid loadings (right) at Node 1, 10 and 20 in a 3-step TSA cycle

Effect of adsorption step time, t_{ads} on purity and recovery

In order to determine the effect of adsorption time step on purity and recovery, simulations were performed at the same conditions as mentioned earlier. Figure 5.5 depicts the fluid phase composition of CO_2 in the bed at the end of adsorption step for the basic 3-step TSA cycle. The adsorption time was varied from 10 seconds to 80 seconds and the purity and recovery of the cycle was determined as shown in Figure 5.7. The fluid phase profile for CO_2 shows that during the adsorption step the bed is getting mostly saturated with the feed which means that the adsorption time is greater than the breakthrough time and CO_2 is being lost in the product stream from the z=L end. To avoid the loss of CO_2 during the adsorption step in this cycle, it would be necessary either to reduce the running time of the adsorption step or the feed velocity. As it can be observed from Figure 5.7 the recovery of the cycle decreases as the time for adsorption increases and the purity increases as the time increases. This happens mainly because for a lower adsorption time, only few moles of the CO_2 are able to leave from the z=L end but as the time increases the bed gets more saturated with the feed and thus a large amount of the CO_2 is lost from the product end which brings down the recovery as low as 51.3% for an adsorption step of 80 secs.

The increase is the purity for the corresponding time of 80 secs is nearly 57.4% which is mainly because more CO_2 is present in the solid phase as shown in Figure 5.6 and as discussed earlier in the fluid phase, increasing the overall composition collected after the heating step with respect to N_2 in the fluid phase.

Since the maximum purity predicted for this feed condition was calculated to be 99.4% and we are only able to achieve 57.4% purity at 51.3% recovery, this shows that the cycle has not be been optimized very well. The main reason that the purity value is so low is because in the given adsorption times, the amount of N_2 in the fluid phase is very high. During the heating step, this N_2 is collected in the product stream along with the CO_2 from z=0 end.

In order to increase the purity of the cycle, it is of prime importance to remove the excess N_2 in the fluid phase after the adsorption step. Since the amount of N_2 would be low in the product stream after the heating step, the purity of CO_2 would be im-

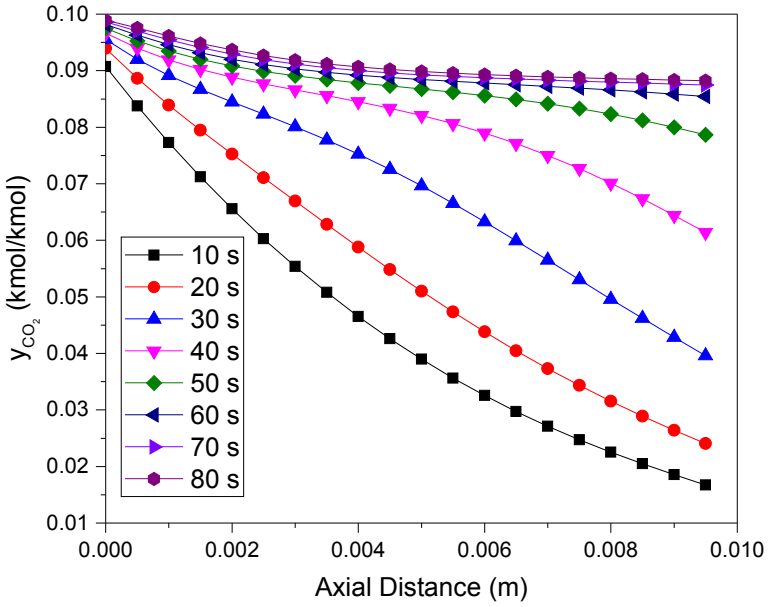

Figure 5.5: Fluid phase CO_2 composition profiles along the bed at the end of different adsorption times

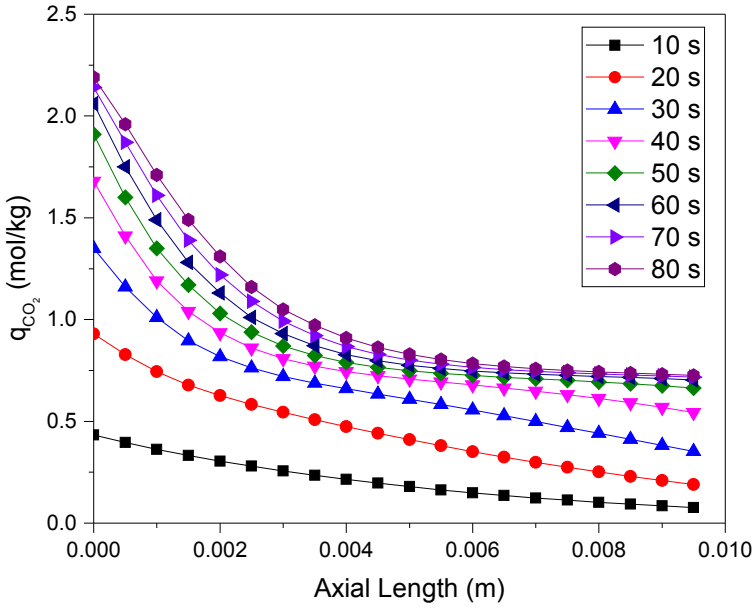

Figure 5.6: Solid phase CO_2 composition profiles along the bed at the end of different adsorption times

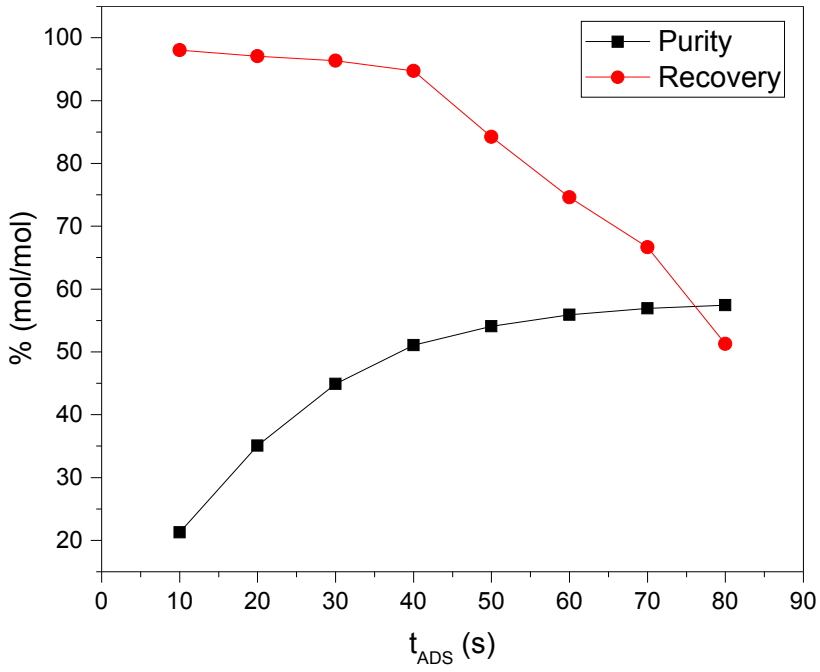

Figure 5.7: CO_2 Purity and Recovery at the end of the cycle for different adsorption times

proved. The excess N_2 can be removed from the bed either with the use of a vacuum or by pushing in steam from the z=0 end and collect N_2 from the z=L end in both the proposed cases. In the next section we have discussed the introduction of this new step and the upgraded 4-step TSA cycle in detail.

5.2.2 4-step TSA Cycle

In this cycle we would like to maximize the purity while trying to maintain a good recovery. We decided on using a steam purge step after the first adsorption step in order to push out the excess N_2 from the product end as shown in Figure 5.8

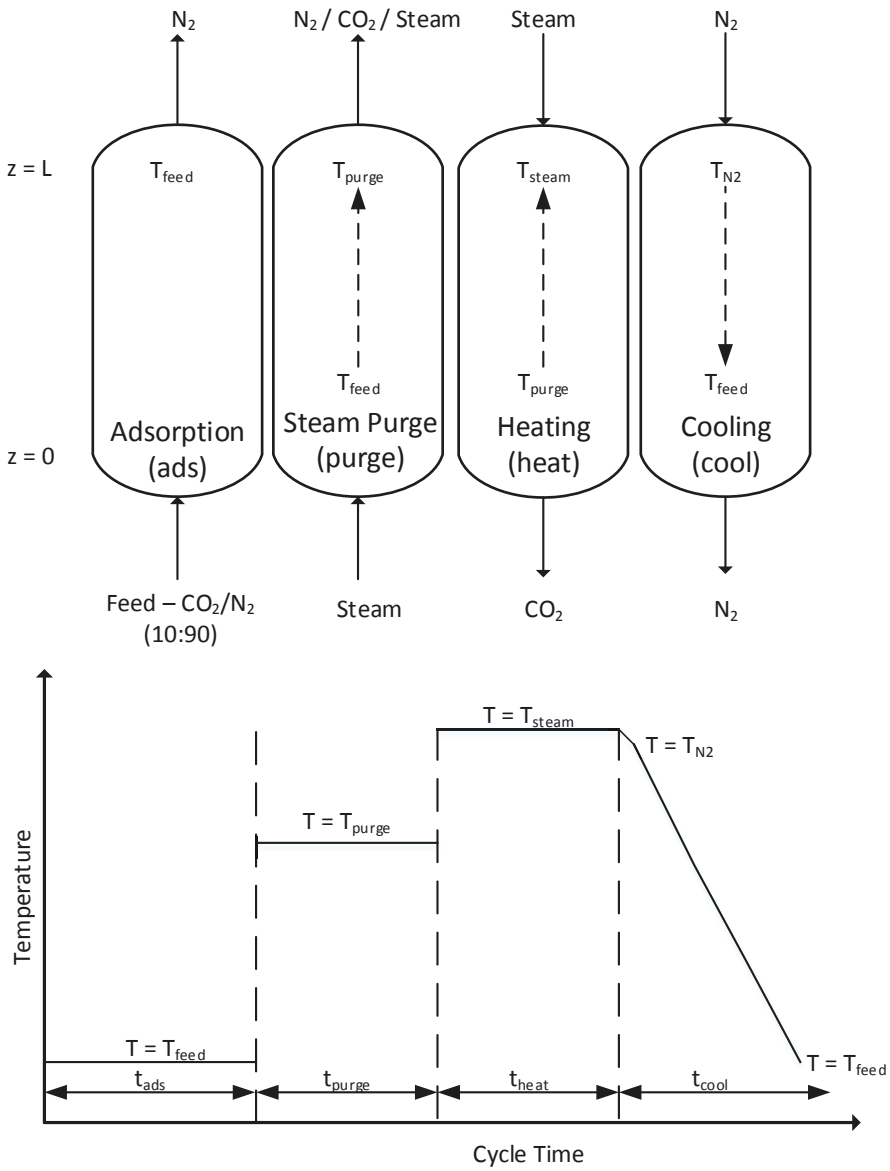

Figure 5.8: 4-step TSA cycle with steam purge step

Purge Step

Steam at 110°C (383.15K) would be fed into the column from z=0 end to drive out N_2 from the product end at z=L. It should be noted that the steam would heat the bed which would cause the CO_2 present in the solid phase to desorb and populate the fluid phase only to be driven out along with N_2. The time span of this step would be crucial in determining the purity and recovery achieved at the end of the cycle. The direct implications of this step would be on the amount of energy required for the overall process as the quantity of steam required would be increased.
The purity of the recovered CO_2 would be maximum when almost all of the N_2 would be pushed out of the bed.

5.2.2.1 Results

The 4-step steam purge cycle was simulated using the same model parameters as mentioned in Table 5.2 until the bed achieved the initial conditions at the end of the cycle. On addition of the purge step, the dynamics of the bed were altered which would affect the purity and recovery. The time for the purge step was initially chosen to be 5 secs and its affect on purity and recovery would be discussed later in the section.

Figure 5.9 shows the increase in temperature across the column during the steam purge step. As it can be observed the increase in temperature is most prevalent at node 1 for the given time and temperature of the steam purge step and other nodes are not much affected. The node 1 at z=0 end is the first to be exposed to the steam and thus gets heated to a temperature of 9696°C from 82°C in 5 seconds and also starts losing CO_2 from the solid phase as shown in Figure 5.10.

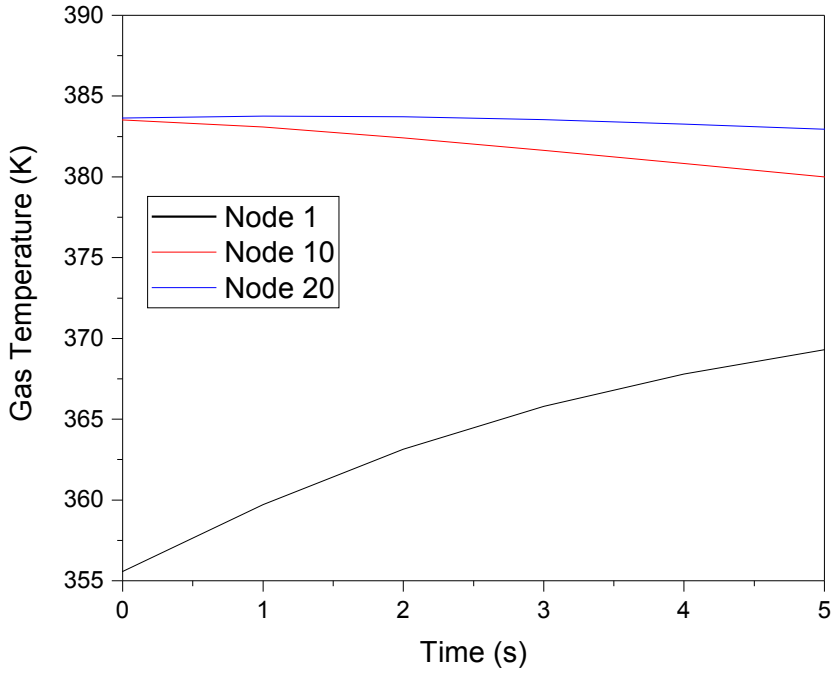

Figure 5.9: Temperature profile across the column during the steam purge

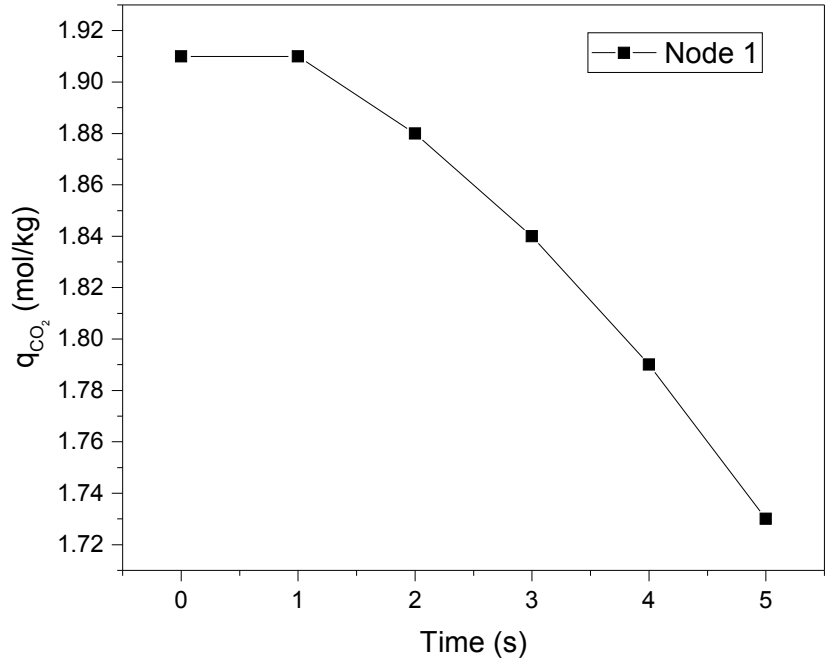

Figure 5.10: Solid phase loading profile at node 1 during the steam purge

Effect of steam purge time step, t_{purge} on purity and recovery

The steam purge time step was varied from 1 second to 15 seconds to determine the effect on purity and recovery. We observed that the purity of CO_2 collected after the heating step increased as the t_{purge} increased and conversely the CO_2 recovery decreased with the increase in t_{purge} as shown in Figure 5.11. The observed trend can

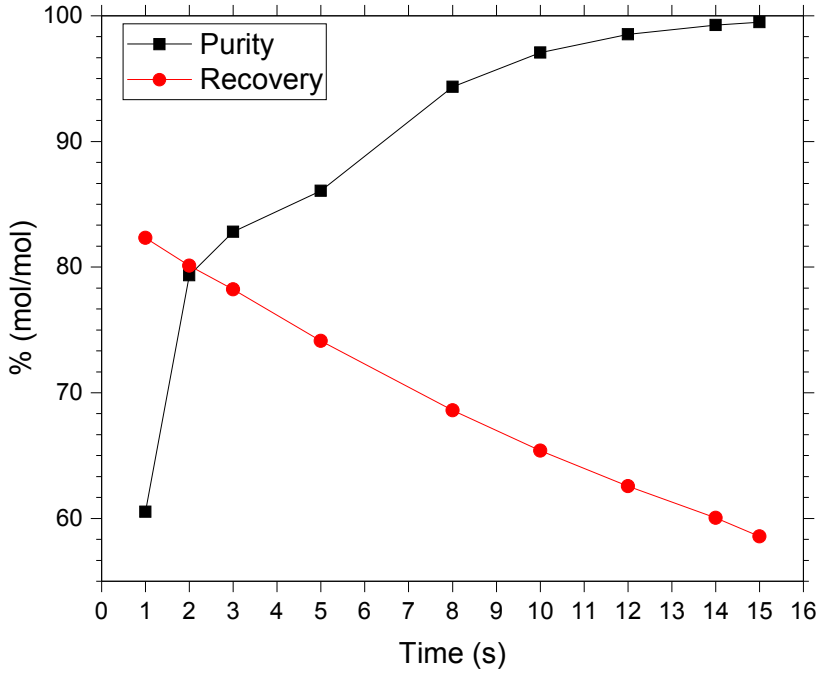

Figure 5.11: CO_2 Purity and Recovery at the end of the 4-step TSA cycle for different adsorption times

be explained using Figure 5.12 in which we can see that as the t_{purge} increases the amount of CO_2 lost in the outlet with respect to the feed increases. As stated earlier due to the steam, temperature of the column would increase causing the CO_2 to desorb and pushed out of the column and as more CO_2 is pushed out, the recovery of the cycle drops. Also it can be seen that the composition of N_2 in the outlet decreases in comparison to CO_2 with t_{purge}, which implies that the amount of N_2 in the column has decreased which ultimately increases the purity as seen in Figure 5.11.

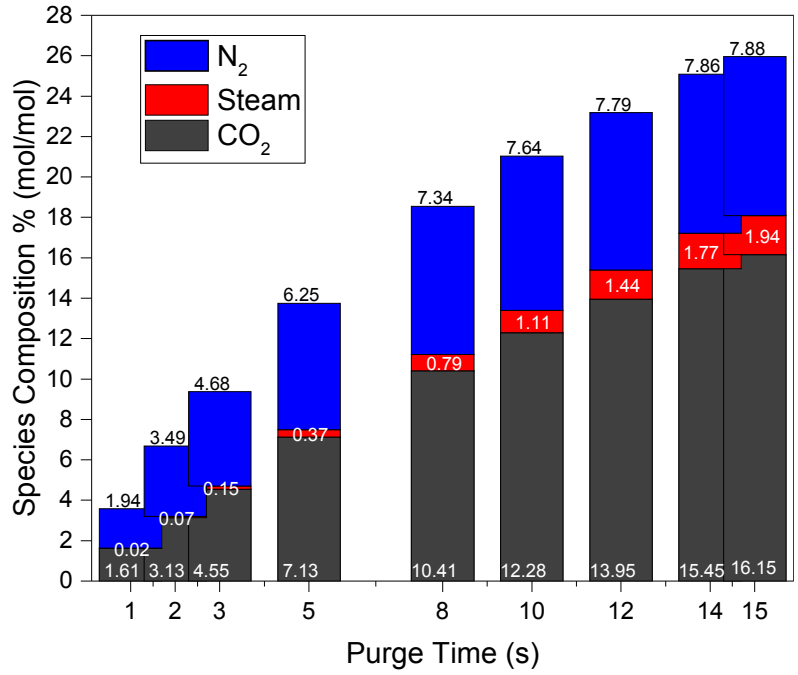

Figure 5.12: Outlet compositions after the steam purge step with respect to the cycle feeds

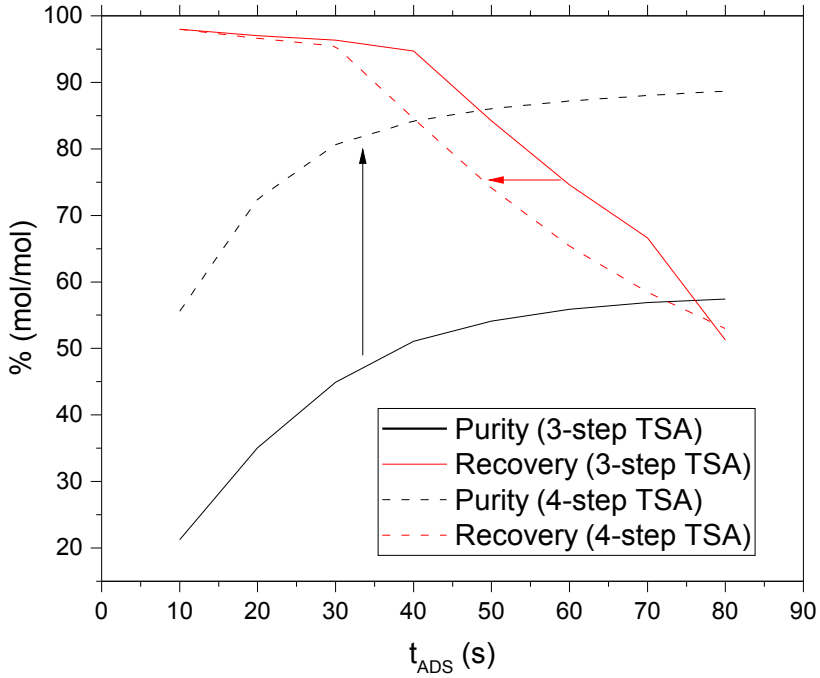

Figure 5.13: Effect of steam purge step on purity and recovery when compared to 3-step TSA cycle

The 4-step cycle with steam purge provides a significant advantage in terms of purity with respect to the 3-step TSA cycle, from 54.1% to 84.2% for a 50 seconds of adsorption step time as depicted in Figure 5.13. The use of steam purge decreases considerably the amount of N_2 collected at the product end of heating step (z=0) by pushing it out of the z=L end in the previous step. The increase in CO_2 purity is accompanied by a decrease in its recovery due to the loss of CO_2 as a result of steam heating and purge in the second step.

5.2.3 Effect of Bed Length on Purity

In order to determine the effect of bed length on purity and recovery, two new beds of height 0.5m and 1.0m and diameters of 0.16m and 0.289m respectively, were developed. A basic 3-step TSA cycle was performed on these beds. The beds had the same parameters as stated in Table 5.2 and were subjected to the same step times as mentioned in Table 5.3, so as to remain consistent with the earlier studies. Only two parameters were altered. the feed velocity v_{feed}, which was increased to 1 m/s and the outside heat transfer coefficient, h_{out}, between the wall and the ambient, was reduced to 0.025 $Jm^{-2}K^{-1}s^{-1}$ so as to provide near adiabatic conditions for the system.

The purity and recovery at the end of the 3-step TSA cycle was evaluated for the

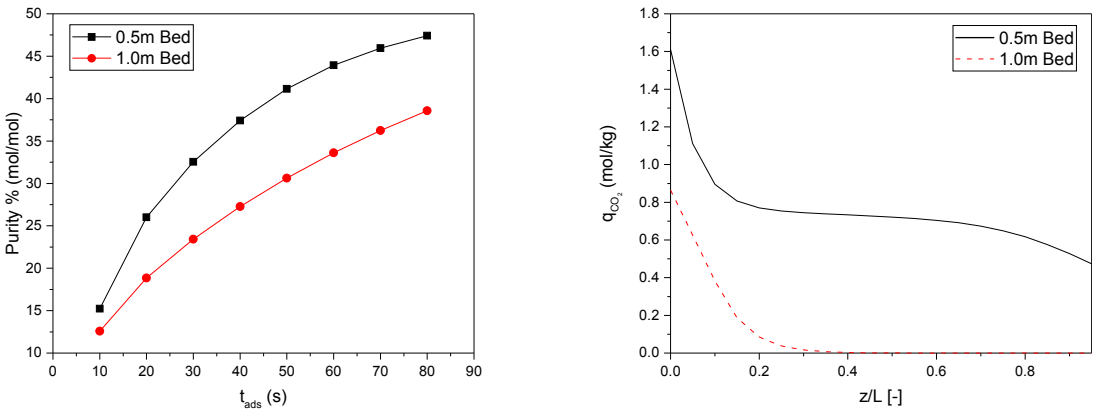

Figure 5.14: Purity (left) and solid phase loadings (right) for the 0.5m and 1.0m beds at the end of adsorption step for t_{ads} = 40 secs

two beds. The adsorption time for this study was also varied from 10 seconds to 80 seconds. As observed earlier the recovery for both the beds was mostly 100% with

negligible difference at different step times and thus was decided to be omitted from this discussion. As seen in Figure 5.14, the purity for both the cases increases with adsorption time, as the beds get saturated with the feed and a higher amount of CO_2 is adsorbed. The purity for 0.5m bed is greater than the 1.0m bed at all times and this effect can be explained using Figure 5.14, in which it is evident that as the 0.5m bed has a higher amount of solid phase loading than the 1.0m bed. Similar observations have been reported in literature [17] where the purity of the strongly adsorbed species reduced with the increase in bed length.

Chapter 6

Concluding Remarks

6.1 Summary and Conclusion

In this work, modeling and process design has been used to evaluate the capability of PEI impregnated silica adsorbents to be used in different TSA cycle configurations developed for the capture of CO_2 from flue gas. Using a 40 wt% impregnated sorbent, experimental measurements of adsorption isotherms at different temperatures were performed. This generated the necessary input parameters for their use in the simulation of cyclic operations developed in this study.

In Chapter 3, results of experimental investigation performed on 40wt% PEI impregnated silica adsorbent were discussed. The adsorbent was loaded in TGA to determine the optimum operating conditions in terms of adsorption and desorption temperatures. It was observed that the sorbent had a maximum adsorption capacity of 2.31 mmol/g at 75°C and 1 bar pressure under simulated flue gas conditions of 10% CO_2 in N_2. The experimental values for equilibrium adsorption capacities at different temperatures were collected for the determination of parameters of single-component adsorption isotherms. The single site Langmuir model was then fitted to the experimental data and the values for maximum saturation capacity, q_s, pre-exponential factor, b_o and heat of adsorption, ΔH_{ads} were determined. The ΔH_{ads} was also determined using the Clausius-Clapeyron equation and the two values were found be in close conjugation with the reported literature values. The experimental

measurements of adsorption isotherms and fitting of single site Langmuir model determined that the temperature swing cycles with adsorption at 75°C and desorption at over 105°C would be the most feasible methodology to capture CO_2 using the amine impregnated adsorbent.

In Chapter 4, the reasons for using Aspen Adsorption as a simulator for modeling the adsorption process were outlined. The different strengths and abilities of the software were presented and the advantages of using the simulator were justified. The model equations used for simulating a rigorous one-dimensional model consisting of mass, momentum and heat balances along with the model assumptions were explicitly detailed. The choice of simulator along with its reliability were validated using the successful implementation of mass, momentum and heat balances in an adsorption process taken from literature. The simulator was able to accurately replicate the column dynamics of the adsorption process for the variables: temperature, velocity and composition. Thus, the developed model was verified and deemed suitable for use in modeling of cyclic adsorption processes.

Chapter 5 dealt with the process design for post-combustion capture using temperature swing adsorption. Firstly, a basic 3-step cycle was designed in which the adsorbent was heated using steam. The cycle configuration and the working of each of the three steps in the cycle were thoroughly explained. The characteristic profiles and transitions observed in the cycle were detailed and further the effect of adsorption time step was studied. Purity and recovery for the 3-step cycle were evaluated at different adsorption time steps and it was observed that the maximum purity attained was quite lower than the maximum theoretical purity. In order to counter this trend and to improve the overall purity of the strongly adsorbed species, an extra stream purge step was added and a new 4-step cycle was implemented. It was determined that the inclusion of the steam purge step greatly increased the purity of the adsorbed species but also lowered the overall recovery of the product. Furthermore, the effect of steam purge time step on purity and recovery was also studied. The effect of bed length on purity and recovery was investigated with development of two beds of variable bed heights and it was observed that the purity decreased as the bed length

increased.

Since the adsorbent is made from amine impregnated silica, which is an inexpensive material with high porosity, large surface area and can be easily produced at a large scale. Therefore, it is worthwhile to produce the adsorbent for CO_2 capture in view of emissions control.

6.2 Future Outlook

Overall, this work has shown that the amine impregnated adsorbent can be successfully used to capture CO_2 using steam as a practical solution for sorbent regeneration. With a rigorous one-dimensional adsorption model, the adsorbent can be tested for application of CO_2 capture; purity and recovery expected for temperature swing adsorption can be predicted. The findings of this research work may provide the basis for future work in post-combustion capture of CO_2 using amine based adsorbents for application in cyclic processes with steam regeneration. Some areas determined based on this study, that can enhance the the impact of amine based sorbents are detailed further.

In the area of experimental investigation, it is of prime importance to determine the equilibrium adsorption capacities of steam at different temperatures for the amine based adsorbents. Breakthrough experiments can also be performed on a scaled up packed bed reactor to generate the necessary information about the isotherms, heat, mass and momentum transfer effects within the column, which can be helpful in understanding and simulating the process better. Efforts must also be made to study the impact of O_2, SO_x and NO_x which are common flue gas components along with CO_2 on the current adsorbent. Single component isotherms generated from this study would give a deeper insight about the application of the adsorbent in an industrial setting.

From the perspective of TSA separation process, new cyclic configurations developed can be compared to the results obtained from the cycles proposed in this study.

Implementation of cycles with feed cooling step so as to reduce the energy consumption for regeneration and use of vacuum in conjugation with steam stripping can be tested which should expectedly lower the cycle times for larger bed sizes. Use of steam for regeneration has been proposed in this study on the basis of easy availability of low pressure steam (as waste heat) in power plants. An actual techno-economic assessment, taking into account the amount of steam consumed and the overall economics of the process when compared to the existing solution in an industrial setting would actually determine the feasibility of this process. Besides, apart from purity and recovery constraints, economics is the major driving force for successful implementation of such technologies in the near future.

Bibliography

[1] Aaron, D., and Tsouris, C. Separation of CO_2 from flue gas: A review. *Separation Science and Technology 40*, 1-3 (2005), 321–348.

[2] Agarwal, A., Biegler, L. T., and Zitney, S. E. Superstructure-based optimal synthesis of pressure swing adsorption cycles for precombustion CO_2 capture. *Industrial & Engineering Chemistry Research 49*, 11 (2010), 5066–5079.

[3] Agarwal, A., Biegler, L. T., and Zitney, S. E. A superstructure-based optimal synthesis of psa cycles for post-combustion CO_2 capture. *AIChE Journal 56*, 7 (2010), 1813–1828.

[4] Agency, I. E. World energy outlook 2007-executive summary. *Head of Communication and Information Office, France* (2007).

[5] Agency, I. E. Technology roadmap: Carbon capture and storage. *Head of Communication and Information Office, France* (2013).

[6] Arenillas, A., Smith, K., Drage, T., and Snape, C. CO_2 capture using some fly ash-derived carbon materials. *Fuel 84*, 17 (2005), 2204 – 2210. Special Issue: The 5th European Conference on Coal Research and its Applications.

[7] Basmadjian, D. On the possibility of omitting the cooling step in thermal gas adsorption cycles. *The Canadian Journal of Chemical Engineering 53*, 2 (1975), 234–238.

[8] Belmabkhout, Y., and Sayari, A. Isothermal versus non-isothermal adsorption- desorption cycling of triamine-grafted pore-expanded MCM-41 mesoporous silica for CO_2 capture from flue gas. *Energy & Fuels 24*, 9 (2010), 5273–5280.

[9] Bonjour, J., Chalfen, J.-B., and Meunier, F. Temperature swing adsorption process with indirect cooling and heating. *Industrial & Engineering Chemistry Research 41*, 23 (2002), 5802–5811.

[10] Burchell, T., Judkins, R., Rogers, M., and Williams, A. A novel process and material for the separation of carbon dioxide and hydrogen sulfide gas mixtures. *Carbon 35*, 9 (1997), 1279 – 1294.

[11] Burdyny, T., and Struchtrup, H. Hybrid membrane/cryogenic separation of oxygen from air for use in the oxy-fuel process. *Energy 35*, 5 (2010), 1884 – 1897.

[12] Caurie, M. Misapplication of the Clausius-Clapeyron equation for estimating heats of adsorption in foods. *International Journal of Food Science & Technology 48*, 3 (2013), 596–600.

[13] Chaffee, A. L. Molecular modeling of HMS hybrid materials for CO_2 adsorption. *Fuel Processing Technology 86*, 1415 (2005), 1473 – 1486. Carbon Dioxide Capture and Sequestration.

[14] Chaffee, A. L., Knowles, G. P., Liang, Z., Zhang, J., Xiao, P., and Webley, P. A. CO_2capture by adsorption: Materials and process development. *International Journal of Greenhouse Gas Control 1*, 1 (2007), 11 – 18. 8th International Conference on Greenhouse Gas Control TechnologiesGHGT-8.

[15] Chaikittisilp, W., Kim, H.-J., and Jones, C. W. Mesoporous alumina-supported amines as potential steam-stable adsorbents for capturing CO_2 from simulated flue gas and ambient air. *Energy & Fuels 25*, 11 (2011), 5528–5537.

[16] Choi, S., Drese, J., and Jones, C. Adsorbent materials for carbon dioxide capture from large anthropogenic point sources. *ChemSusChem 2*, 9 (2009), 796–854.

[17] Chou, C.-t., Huang, C.-h., Cheng, N.-c., Shen, Y.-t., Yang, H.-s., and Yang, M.-W. Adsorption processes for CO_2 capture from flue gas using polyaniline solid sorbent. *RSC Adv. 4* (2014), 36307–36315.

[18] Clausse, M., Merel, J., and Meunier, F. Numerical parametric study on CO_2 capture by indirect thermal swing adsorption. *International Journal of Greenhouse Gas Control 5*, 5 (2011), 1206 – 1213.

[19] Cloirec, P. L. Adsorption onto activated carbon fiber cloth and electrothermal desorption of volatile organic compound (vocs): A specific review. *Chinese Journal of Chemical Engineering 20*, 3 (2012), 461 – 468.

[20] D'Alessandro, D., Smit, B., and Long, J. Carbon dioxide capture: Prospects for new materials. *Angewandte Chemie International Edition 49*, 35 (2010), 6058–6082.

[21] Dasgupta, S., Nanoti, A., Gupta, P., Jena, D., Goswami, A. N., and Garg, M. O. Carbon di-oxide removal with mesoporous adsorbents in a single column pressure swing adsorber. *Sep. Sci. Technol. 44*, 16 (2009), 3973–3983.

[22] Delgado, J. A., Uguina, M. A., Sotelo, J. L., Augueda, V. I., Sanz, A., and Gomez, P. Numerical analysis of CO_2 concentration and recovery from flue gas by a novel vacuum swing adsorption cycle. *Computers & Chemical Engineering 35*, 6 (2011), 1010 – 1019.

[23] Diagne, D., Goto, M., and Hirose, T. New psa process with intermediate feed inlet position operated with dual refluxes: application to carbon dioxide removal and enrichment. *Journal of Chemical Engineering of Japan* (1994).

[24] Diagne, D., Goto, M., and Hirose, T. Parametric studies on CO_2 separation and recovery by a dual reflux psa process consisting of both rectifying and stripping sections. *Industrial and Engineering Chemistry Research* (1995).

[25] Dlugokencky, E., and Tans, P. Trends in atmospheric carbon dioxide, August 2015.

[26] Do, D. D. *Adsorption Analysis: Equilibria and Kinetics*, vol. 2 of *Chemical Engineer Series*. Imperial College Press, 1998.

[27] Dombrowski, K. D., Lehmann, C. M. B., Sullivan, P. D., Ramirez, D., and Rood, Mark J. adn Hay, K. J. Organic vapor recovery and energy efficiency during electric regeneration of an activated carbon fiber cloth adsorber. *Journal of Environmental Engineering 130*, 3 (2004), 268–275.

[28] Drage, T., Arenillas, A., Smith, K., and Snape, C. Thermal stability of polyethylenimine based carbon dioxide adsorbents and its influence on selection of regeneration strategies. *Microporous and Mesoporous Materials 116*, 13 (2008), 504 – 512.

[29] Drese, J. H., Choi, S., Lively, R. P., Koros, W. J., Fauth, D. J., Gray, M. L., and Jones, C. W. Synthesis, structure and property relationships for hyperbranched aminosilica CO_2 adsorbents. *Advanced Functional Materials 19*, 23 (2009), 3821–3832.

[30] Dutcher, B., Adidharma, H., and Radosz, M. Carbon filter process for flue-gas carbon capture on carbonaceous sorbents: Steam-aided vacuum swing adsorption option. *Industrial & Engineering Chemistry Research 50*, 16 (2011), 9696–9703.

[31] Dutcher, B., Krutkramelis, K., Adidharma, H., and Radosz, M. Carbon filter process for flue-gas carbon capture on carbonaceous sorbents: field tests of steam-aided vacuum swing adsorption. *Energy & Fuels 26*, 4 (2012), 2539–2545.

[32] Ebner, A., and Ritter, J. Equilibrium theory analysis of dual reflux psa for separation of a binary mixture. *AIChE Journal 50*, 10 (2004), 2418–2429. cited By 17.

[33] Ebner, A. D., Gray, M. L., Chisholm, N. G., Black, Q. T., Mumford, D. D., Nicholson, M. A., and Ritter, J. A. Suitability of a solid amine sorbent for CO_2 capture by pressure swing adsorption. *Industrial & Engineering Chemistry Research 50*, 9 (2011), 5634–5641.

[34] Fauth, D., Gray, M., Pennline, H., Krutka, H., Sjostrom, S., and Ault, A. Investigation of porous silica supported mixed-amine sorbents for post-combustion CO_2 capture. *Energy & Fuels 26*, 4 (2012), 2483–2496.

[35] Fauth, D. J., Frommell, E. A., Hoffman, J. S., Reasbeck, R. P., and Pennline, H. W. Eutectic salt promoted lithium zirconate: Novel high temperature sorbent for CO_2 capture. *Fuel Processing Technology 86*, 1415 (2005), 1503 – 1521. Carbon Dioxide Capture and Sequestration.

[36] Figueroa, J. D., Fout, T., Plasynski, S., McIlvried, H., and Srivastava, R. D. Advances in CO_2 capture technology: The u.s. department of energy's carbon sequestration program. *International Journal of Greenhouse Gas Control 2*, 1 (2008), 9 – 20.

[37] Filburn, T., Helble, J. J., and Weiss, R. A. Development of supported ethanolamines and modified ethanolamines for CO_2 capture. *Industrial & Engineering Chemistry Research 44*, 5 (2005), 1542–1546.

[38] Fisher, J. C., Tanthana, J., and Chuang, S. S. Oxide-supported tetraethylenepentamine for CO_2 capture. *Environmental Progress & Sustainable Energy 28*, 4 (2009), 589–598.

[39] GISTEMP, T. GISS surface temperature analysis (GISTEMP), August 2015.

[40] GISTEMP, T. NASA, NOAA find 2014 warmest year in modern record GISS surface temperature analysis (GISTEMP), August 2015.

[41] Grande, C. A., Ribeiro, R. P., Oliveira, E. L., and Rodrigues, A. E. Electric swing adsorption as emerging CO_2 capture technique. *Energy Procedia 1*, 1 (2009), 1219 – 1225. Greenhouse Gas Control Technologies 9Proceedings of the 9th International Conference on Greenhouse Gas Control Technologies (GHGT-9), 1620 November 2008, Washington DC, USA.

[42] Grande, C. A., and Rodrigues, A. E. Electric swing adsorption for CO_2 removal from flue gases. *International Journal of Greenhouse Gas Control 2*, 2 (2008), 194 – 202.

[43] Gray, M., Hoffman, J., Hreha, D., Fauth, D., Hedges, S., Champagne, K., and Pennline, H. Parametric study of solid amine sorbents for the capture of carbon dioxide. *Energy & Fuels 23*, 10 (2009), 4840–4844.

[44] Haghpanah, R., Majumder, A., Nilam, R., Rajendran, A., Farooq, S., Karimi, I. A., and Amanullah, M. Multiobjective optimization of a four-step adsorption process for postcombustion CO_2 capture via finite volume simulation. *Industrial & Engineering Chemistry Research 52*, 11 (2013), 4249–4265.

[45] Hammache, S., Hoffman, J. S., Gray, M. L., Fauth, D. J., Howard, B. H., and Pennline, H. W. Comprehensive study of the impact of steam on polyethyleneimine on silica for CO_2 capture. *Energy & Fuels 27*, 11 (2013), 6899–6905.

[46] Harlick, P. J. E., and Sayari, A. Applications of pore-expanded mesoporous silica. 5. triamine grafted material with exceptional CO_2 dynamic and equilibrium adsorption performance. *Industrial & Engineering Chemistry Research 46*, 2 (2007), 446–458.

[47] Hasan, M. M. F., Baliban, R. C., Elia, J. A., and Floudas, C. A. Modeling, simulation, and optimization of postcombustion co2 capture for variable feed concentration and flow rate. 2. pressure swing adsorption and vacuum swing adsorption processes. *Industrial & Engineering Chemistry Research 51*, 48 (2012), 15665–15682.

[48] Hedin, N., Andersson, L., Bergstrom, L., and Yan, J. Adsorbents for the post-combustion capture of CO_2 using rapid temperature swing or vacuum swing adsorption. *Applied Energy 104*, 0 (2013), 418 – 433.

[49] Heydari-Gorji, A., and Sayari, A. Thermal, oxidative, and co2-induced degradation of supported polyethylenimine adsorbents. *Industrial & Engineering Chemistry Research 51*, 19 (2012), 6887–6894.

[50] Heydari-Gorji, A., Yang, Y., and Sayari, A. Effect of the pore length on CO_2 adsorption over amine-modified mesoporous silicas. *Energy & Fuels 25*, 9 (2011), 4206–4210.

[51] Hicks, J. C., Drese, J. H., Fauth, D. J., Gray, M. L., Qi, G., and Jones, C. W. Designing adsorbents for CO_2 capture from flue gas-hyperbranched aminosilicas capable of capturing co2 reversibly. *J. Am. Chem. Soc. 130*, 10 (2008), 2902–2903. PMID: 18281986.

[52] Hiyoshi, N., Yogo, K., and Yashima, T. Adsorption of carbon dioxide on amine modified sba-15 in the presence of water vapor. *Chemistry Letters 33*, 5 (2004), 510–511.

[53] Hiyoshi, N., Yogo, K., and Yashima, T. Adsorption characteristics of carbon dioxide on organically functionalized sba-15. *Microporous and Mesoporous Materials 84*, 13 (2005), 357 – 365.

[54] Ho, M. T., Allinson, G. W., and Wiley, D. E. Reducing the cost of CO_2 capture from flue gases using pressure swing adsorption. *Industrial & Engineering Chemistry Research 47*, 14 (2008), 4883–4890.

[55] Jadhav, P. D., Chatti, R. V., Biniwale, R. B., Labhsetwar, N. K., Devotta, S., and Rayalu, S. S. Monoethanol amine modified zeolite 13x for co2 adsorption at different temperatures. *Energy & Fuels 21*, 6 (2007), 3555–3559.

[56] Joss, L., Gazzani, M., Hefti, M., Marx, D., and Mazzotti, M. Temperature swing adsorption for the recovery of the heavy component: An equilibrium-based shortcut model. *Industrial & Engineering Chemistry Research 54*, 11 (2015), 3027–3038.

[57] Jung, H., Jo, D. H., Lee, C. H., Chung, W., Shin, D., and Kim, S. H. Carbon dioxide capture using poly(ethylenimine)-impregnated poly(methyl methacrylate)-supported sorbents. *Energy & Fuels 28*, 6 (2014), 3994–4001.

[58] Khatri, R. A., Chuang, S. S. C., Soong, Y., and Gray, M. Carbon dioxide capture by diamine-grafted sba-15: A combined fourier transform infrared and mass spectrometry study. *Industrial & Engineering Chemistry Research 44*, 10 (2005), 3702–3708.

[59] Khatri, R. A., Chuang, S. S. C., Soong, Y., and Gray, M. Thermal and chemical stability of regenerable solid amine sorbent for CO_2 capture. *Energy & Fuels 20*, 4 (2006), 1514–1520.

[60] Kikkinides, E. S., Yang, R. T., and Cho, S. H. Concentration and recovery of carbon dioxide from flue gas by pressure swing adsorption. *Industrial & Engineering Chemistry Research 32*, 11 (1993), 2714–2720.

[61] Knofel, C., Descarpentries, J., Benzaouia, A., Zelek, V., Mornet, S., Llewellyn, P., and Hornebecq, V. Functionalised micro-/mesoporous silica for the adsorption of carbon dioxide. *Microporous and Mesoporous Materials 99*, 12 (2007), 79 – 85. Inside Pores Workshop In Situ Study and Development of Processes Involving NanoPorous Solids.

[62] Knowles, G. P., Delaney, S. W., and Chaffee, A. L. Amine-functionalised mesoporous silicas as CO_2 adsorbents. In *Nanoporous Materials IVProceedings of the 4th International Symposium on Nanoporous Materials*, A. Sayari and M. Jaroniec, Eds., vol. 156 of *Studies in Surface Science and Catalysis*. Elsevier, 2005, pp. 887 – 896.

[63] Knowles, G. P., Delaney, S. W., and Chaffee, A. L. Diethylenetriamine[propyl(silyl)]-functionalized (DT) mesoporous silicas as CO_2 adsorbents. *Industrial & Engineering Chemistry Research 45*, 8 (2006), 2626–2633.

[64] Knowles, G. P., Graham, J. V., Delaney, S. W., and Chaffee, A. L. Aminopropyl-functionalized mesoporous silicas as CO_2 adsorbents. *Fuel Pro-*

cessing Technology 86, 1415 (2005), 1435 – 1448. Carbon Dioxide Capture and Sequestration.

[65] Ko, D., Siriwardane, R., and Biegler, L. T. Optimization of a pressure-swing adsorption process using zeolite 13x for CO_2 sequestration. *Industrial & Engineering Chemistry Research 42*, 2 (2003), 339–348.

[66] Ko, D., Siriwardane, R., and Biegler, L. T. Optimization of pressure swing adsorption and fractionated vacuum pressure swing adsorption processes for CO_2 capture. *Industrial & Engineering Chemistry Research 44*, 21 (2005), 8084–8094.

[67] Leal, O., Bolivar, C., Ovalles, C., Garcia, J. J., and Espidel, Y. Reversible adsorption of carbon dioxide on amine surface-bonded silica gel. *Inorganica Chimica Acta 240*, 12 (1995), 183 – 189.

[68] Leung, D. Y., Caramanna, G., and Maroto-Valer, M. M. An overview of current status of carbon dioxide capture and storage technologies. *Renewable and Sustainable Energy Reviews 39*, 0 (2014), 426 – 443.

[69] Li, W., Bollini, P., Didas, S. A., Choi, S., Drese, J. H., and Jones, C. W. Structural changes of silica mesocellular foam supported amine-functionalized co2 adsorbents upon exposure to steam. *ACS Applied Materials & Interfaces 2*, 11 (2010), 3363–3372. PMID: 21062035.

[70] Li, W., Choi, S., Drese, J., Hornbostel, M., Krishnan, G., Eisenberger, P., and Jones, C. Steam-stripping for regeneration of supported amine-based CO_2 adsorbents. *ChemSusChem 3*, 8 (2010), 899–903.

[71] Luo, L., Ramirez, D., Rood, M. J., Grevillot, G., Hay, K. J., and Thurston, D. L. Adsorption and electrothermal desorption of organic vapors using activated carbon adsorbents with novel morphologies. *Carbon 44*, 13 (2006), 2715 – 2723.

[72] Ma, X., Wang, X., and Song, C. "molecular basket" sorbents for separation of CO_2 and H_2S from various gas streams. *J. Am. Chem. Soc. 131*, 16 (2009), 5777–5783. PMID: 19348482.

[73] MacDowell, N., Florin, N., Buchard, A., Hallett, J., Galindo, A., Jackson, G., Adjiman, C. S., Williams, C. K., Shah, N., and Fennell, P. An overview of co_2 capture technologies. *Energy Environ. Sci. 3* (2010), 1645–1669.

[74] Maroto-Valer, M. M., Lu, Z., Zhang, Y., and Tang, Z. Sorbents for CO_2 capture from high carbon fly ashes. *Waste Management 28*, 11 (2008), 2320 – 2328.

[75] Merel, J., Clausse, M., and Meunier, F. Carbon dioxide capture by indirect thermal swing adsorption using 13x zeolite. *Environmental Progress 25*, 4 (2006), 327–333.

[76] Merel, J., Clausse, M., and Meunier, F. Experimental investigation on CO_2 post-combustion capture by indirect thermal swing adsorption using 13x and 5a zeolites. *Industrial & Engineering Chemistry Research 47*, 1 (2008), 209–215.

[77] Metz, B., Davidson, O., Bosch, P., Dave, R., and Meyer, L. Climate change 2007: Mitigation of climate change. *Contribution of Working Group III to the Fourth Assessment Report of the Intergovernmental Panel on Climate*

Change Cambridge University Press, Cambridge, United Kingdom and New York, NY, USA. (2007).

[78] Nilchan, S., and Pantelides, C. On the optimisation of periodic adsorption processes. *Adsorption 4*, 2 (1998), 113–147.

[79] Olajire, A. A. CO_2 capture and separation technologies for end-of-pipe applications - a review. *Energy 35*, 6 (2010), 2610 – 2628. 7th International Conference on Sustainable Energy Technologies 7th International Conference on Sustainable Energy Technologies.

[80] Park, J.-H., Beum, H.-T., Kim, J.-N., and Cho, S.-H. Numerical analysis on the power consumption of the psa process for recovering CO_2 from flue gas. *Industrial and Engineering Chemistry Research 41*, 16 (2002), 4122–4131. cited By 66.

[81] Pirngruber, G. D., Guillou, F., Gomez, A., and Clausse, M. A theoretical analysis of the energy consumption of post-combustion CO_2 capture processes by temperature swing adsorption using solid sorbents. *International Journal of Greenhouse Gas Control 14* (2013), 74 – 83.

[82] Plaza, M., Pevida, C., Arias, B., Fermoso, J., Casal, M., Martn, C., Rubiera, F., and Pis, J. Development of low-cost biomass-based adsorbents for postcombustion CO_2 capture. *Fuel 88*, 12 (2009), 2442 – 2447. 7th European Conference on Coal Research and Its Applications.

[83] Qi, G., Wang, Y., Estevez, L., Duan, X., Anako, N., Park, A.-H. A., Li, W., Jones, C. W., and Giannelis, E. P. High efficiency nanocomposite sorbents for CO_2 capture based on amine-functionalized mesoporous capsules. *Energy Environ. Sci. 4* (2011), 444–452.

[84] Resnik, K., Yeh, J., and Pennline, H. Aqua ammonia process for simultaneous removal of CO_2, SO_2 and NO_x. *International Journal of Environmental Technology and Management 4*, 1-2 (2004), 89–104. cited By 102.

[85] Ribeiro, R. P. P. L., Grande, C. A., and Rodrigues, A. E. Electric swing adsorption for gas separation and purification: A review. *Separation Science and Technology 49*, 13 (2014), 1985–2002.

[86] Ruthven, D. M. *Principles of adsorption and adsorption processes*. John Wiley & Sons, 1984.

[87] Ruthven, D. M. *Adsorption, Fundamentals*. John Wiley & Sons, Inc., 2000.

[88] Sakwa-Novak, M. A., and Jones, C. W. Steam induced structural changes of a poly(ethylenimine) impregnated - alumina sorbent for CO_2 extraction from ambient air. *ACS Applied Materials & Interfaces 6*, 12 (2014), 9245–9255. PMID: 24896554.

[89] Samanta, A., Zhao, A., Shimizu, G. K. H., Sarkar, P., and Gupta, R. Post-combustion CO_2 capture using solid sorbents: A review. *Industrial & Engineering Chemistry Research 51*, 4 (2012), 1438–1463.

[90] Sandhu, N. K. Steam regeneration of amine impregnated silica based sorbents for post combustion capture. Master's thesis, University of Alberta, 2014.

[91] Sanz, R., Calleja, G., Arencibia, A., and Sanz-Prez, E. Co_2 adsorption on branched polyethyleneimine-impregnated mesoporous silica sba-15. *Applied Surface Science 256*, 17 (2010), 5323 – 5328. Seventh International

Symposium Effects of Surface Heterogeneity in Adsorption and Catalysis on Solids - ISSHAC-7.

[92] Sayari, A., Belmabkhout, Y., and Serna-Guerrero, R. Flue gas treatment via CO_2 adsorption. *Chemical Engineering Journal 171*, 3 (2011), 760 – 774. Special Section: Symposium on Post-Combustion Carbon Dioxide Capture.

[93] Serna-Guerrero, R., Belmabkhout, Y., and Sayari, A. Influence of regeneration conditions on the cyclic performance of amine-grafted mesoporous silica for CO_2 capture: An experimental and statistical study. *Chemical Engineering Science 65*, 14 (2010), 4166 – 4172.

[94] Serna-Guerrero, R., Belmabkhout, Y., and Sayari, A. Triamine-grafted pore-expanded mesoporous silica for co_2 capture: Effect of moisture and adsorbent regeneration strategies. *Adsorption 16*, 6 (2010), 567–575.

[95] Shen, C., Liu, Z., Li, P., and Yu, J. Two-stage vpsa process for CO_2 capture from flue gas using activated carbon beads. *Industrial & Engineering Chemistry Research 51*, 13 (2012), 5011–5021.

[96] Shen, C., Yu, J., Li, P., Grande, C., and Rodrigues, A. Capture of CO_2 from flue gas by vacuum pressure swing adsorption using activated carbon beads. *Adsorption 17*, 1 (2011), 179–188.

[97] Sjostrom, S., and Krutka, H. Evaluation of solid sorbents as a retrofit technology for co_2 capture. *Fuel 89*, 6 (2010), 1298 – 1306. Advanced Fossil Energy Utilization.

[98] Skarstrom, C. Method and apparatus for fractionating gaseous mixtures by adsorption, July 12 1960. US Patent 2,944,627.

[99] Smith, O. J., and Westerberg, A. W. The optimal design of pressure swing adsorption systems. *Chemical Engineering Science 46*, 12 (1991), 2967 – 2976.

[100] Son, W.-J., Choi, J.-S., and Ahn, W.-S. Adsorptive removal of carbon dioxide using polyethyleneimine-loaded mesoporous silica materials. *Microporous and Mesoporous Materials 113*, 13 (2008), 31 – 40.

[101] Son, W.-J., Choi, J.-S., and Ahn, W.-S. Adsorptive removal of carbon dioxide using polyethyleneimine-loaded mesoporous silica materials. *Microporous and Mesoporous Materials 113*, 13 (2008), 31 – 40.

[102] Starns, T., Sjostrom, S., Krutka, H., Wilson, C., and Ivie, M. Solid sorbents as a retrofit co_2 capture technology: Update on 1 mwe pilot progress. Tech. rep., Paper 2012-A-53-MEGA-Air and Waste Management Association, Baltimore, MD, Aug. 20- 23, 2012.

[103] Tarka, T. J., Ciferno, J. P., Gray, M. L., and Fauth, D. J. Co_2 capture systems utilizing amine enhanced solid sorbents. In *Fifth Annual Conference on Carbon Capture & Sequestration* (Alexandria, VA, May 2006), no. Paper 152.

[104] Wang, K., Shang, H., Li, L., Yan, X., Yan, Z., Liu, C., and Zha, Q. Efficient co_2 capture on low-cost silica gel modified by polyethyleneimine. *Journal of Natural Gas Chemistry 21*, 3 (2012), 319 – 323.

[105] Wang, Q., Luo, J., Zhong, Z., and Borgna, A. CO_2 capture by solid adsorbents and their applications: Current status and new trends. *Energy Environ. Sci. 4* (2011), 42–55.

[106] Webley, P. A. Adsorption technology for CO_2 separation and capture: a perspective. *Adsorption 20*, 2-3 (2014), 225–231.

[107] Wilfong, W. C., Kail, B. W., and Gray, M. L. Rapid screening of immobilized amine CO_2 sorbents for steam stability by their direct contact with liquid h2o. *ChemSusChem 8*, 12 (2015), 2041–2045.

[108] Xiao, P., Zhang, J., Webley, P., Li, G., Singh, R., and Todd, R. Capture of CO_2 from flue gas streams with zeolite 13x by vacuum-pressure swing adsorption. *Adsorption 14*, 4-5 (2008), 575–582.

[109] Xu, X., Song, C., Andresen, J. M., Miller, B. G., and Scaroni, A. W. Novel polyethylenimine-modified mesoporous molecular sieve of MCM-41 type as high-capacity adsorbent for co2 capture. *Energy & Fuels 16*, 6 (2002), 1463–1469.

[110] Xu, X., Song, C., Andrsen, J. M., Miller, B. G., and Scaroni, A. W. Preparation and characterization of novel CO_2 molecular basket adsorbents based on polymer-modified mesoporous molecular sieve mcm-41. *Microporous Mesoporous Mater. 62*, 12 (2003), 29 – 45.

[111] Yeh, J. T., Resnik, K. P., Rygle, K., and Pennline, H. W. Semi-batch absorption and regeneration studies for CO_2 capture by aqueous ammonia. *Fuel Processing Technology 86*, 1415 (2005), 1533 – 1546. Carbon Dioxide Capture and Sequestration.

[112] Yu, C.-H., Huang, C.-H., and Tan, C.-S. A review of CO_2 capture by absorption and adsorption. *Aerosol and Air Quality Research 12*, 5 (2012), 745–769.

[113] Yu, F. D., Luo, L., and Grevillot, G. Electrothermal swing adsorption of toluene on an activated carbon monolith: Experiments and parametric theoretical study. *Chemical Engineering and Processing: Process Intensification 46*, 1 (2007), 70 – 81.

[114] Zhang, J., and Webley, P. A. Cycle development and design for CO_2 capture from flue gas by vacuum swing adsorption. *Environmental Science & Technology 42*, 2 (2008), 563–569. PMID: 18284163.

[115] Zhang, J., Webley, P. A., and Xiao, P. Effect of process parameters on power requirements of vacuum swing adsorption technology for CO_2 capture from flue gas. *Energy Conversion and Management 49*, 2 (2008), 346 – 356.

[116] Zhao, A., Samanta, A., Sarkar, P., and Gupta, R. Carbon dioxide adsorption on amine-impregnated mesoporous sba-15 sorbents: Experimental and kinetics study. *Industrial & Engineering Chemistry Research 52*, 19 (2013), 6480–6491.

[117] Zhao, W., Zhang, Z., Li, Z., and Cai, N. Investigation of thermal stability and continuous CO_2 capture from flue gases with supported amine sorbent. *Industrial & Engineering Chemistry Research 52*, 5 (2013), 2084–2093.

Appendix A

Adsorption Data on PEI-impregnated Silica

A.1 CO_2 adsorption data

Table A.1: Experimental equilibrium data for CO_2 on PEI-impregnated silica adsorbent at 60°C,75°C, 90°C and 105°C.

	60°C	**75°C**	**90°C**	**105°C**
$\mathbf{P_{CO_2}}$ [bar]	$\mathbf{q_{CO_2}}$ [mol kg^{-1}]	$\mathbf{q_{CO_2}}$ [mol kg^{-1}]	$\mathbf{q_{CO_2}}$ [mol kg^{-1}]	$\mathbf{q_{CO_2}}$ [mol kg^{-1}]
0.015	0.44	1.33	0.34	0.035
0.02	1.25	1.57	0.77	0.10
0.035	1.85	1.94	1.41	0.39
0.05	1.96	2.01	1.64	0.75
0.075	2.06	2.20	1.89	1.13
0.1	2.13	2.31	2.03	1.47
0.2	2.23	2.45	2.05	1.72
0.4	2.35	2.61	2.21	1.95
0.6	2.46	2.62	2.43	2.06
0.8	2.51	2.62	2.44	2.19
1	2.65	2.86	2.60	2.31

A.2 N_2 adsorption

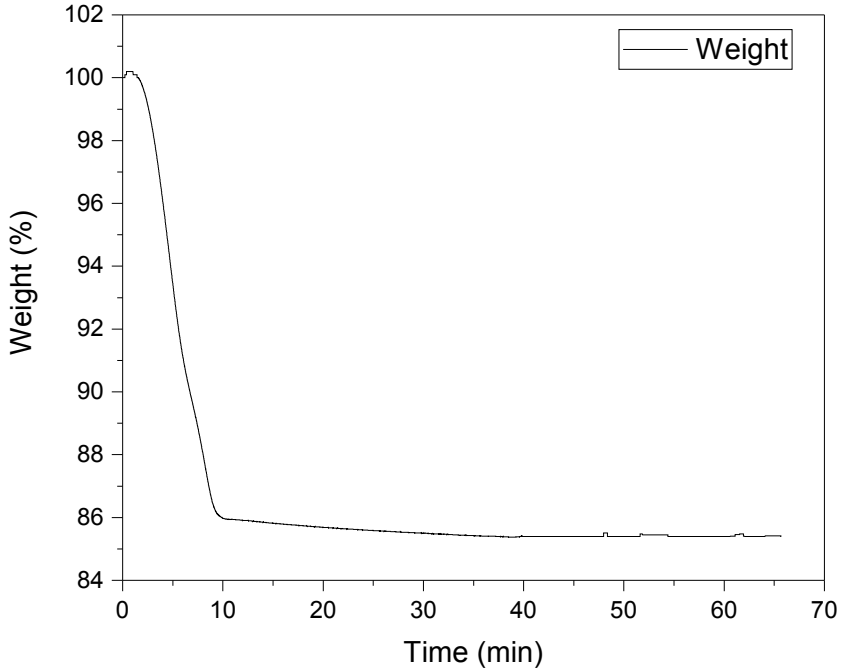

Figure A.1: Pure N_2 TGA analysis curve at 75°C

Appendix B

ASPEN Adsorption Flowsheet

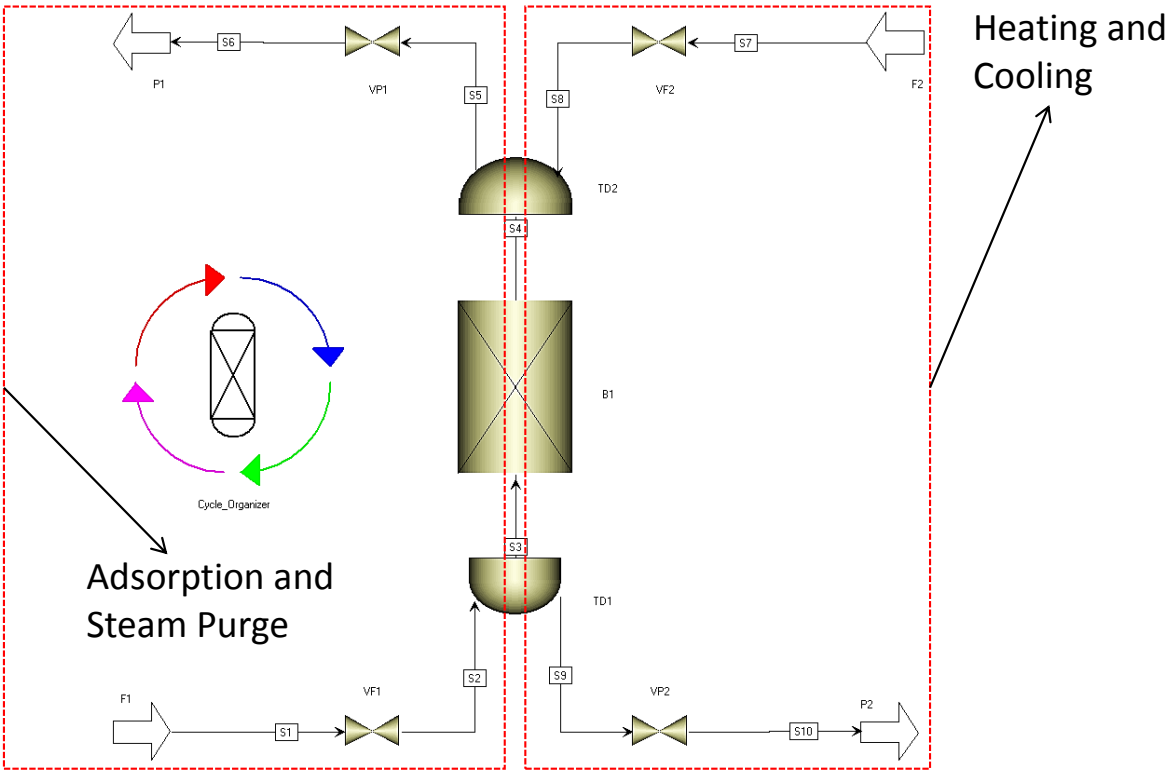

Figure B.1: ASPEN adsorption flow sheet for the 3-step and the 4-step TSA cycle

Appendix C

3-step TSA for 0.5m Bed

Table C.1: Process conditions(step times and stream temperatures) for the 3-step TSA cycle configuration in a 0.5m Bed

	t_{ads} [min]	t_{heat} [min]	t_{cool} [min]	T_{feed} [K]	T_{steam} [K]	T_{N_2} [K]
3-step cycle [0.5m Bed]	10	155	120	378.15	403.15	398.15

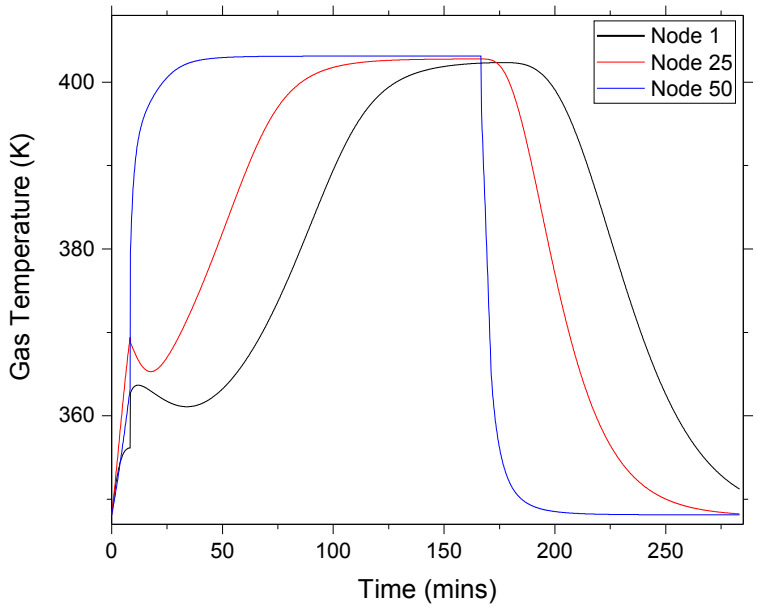

Figure C.1: Gas temperatures at Node 1, 10 and 20 at the end of adsorption step in a 3-step TSA cycle for a 0.5m Bed

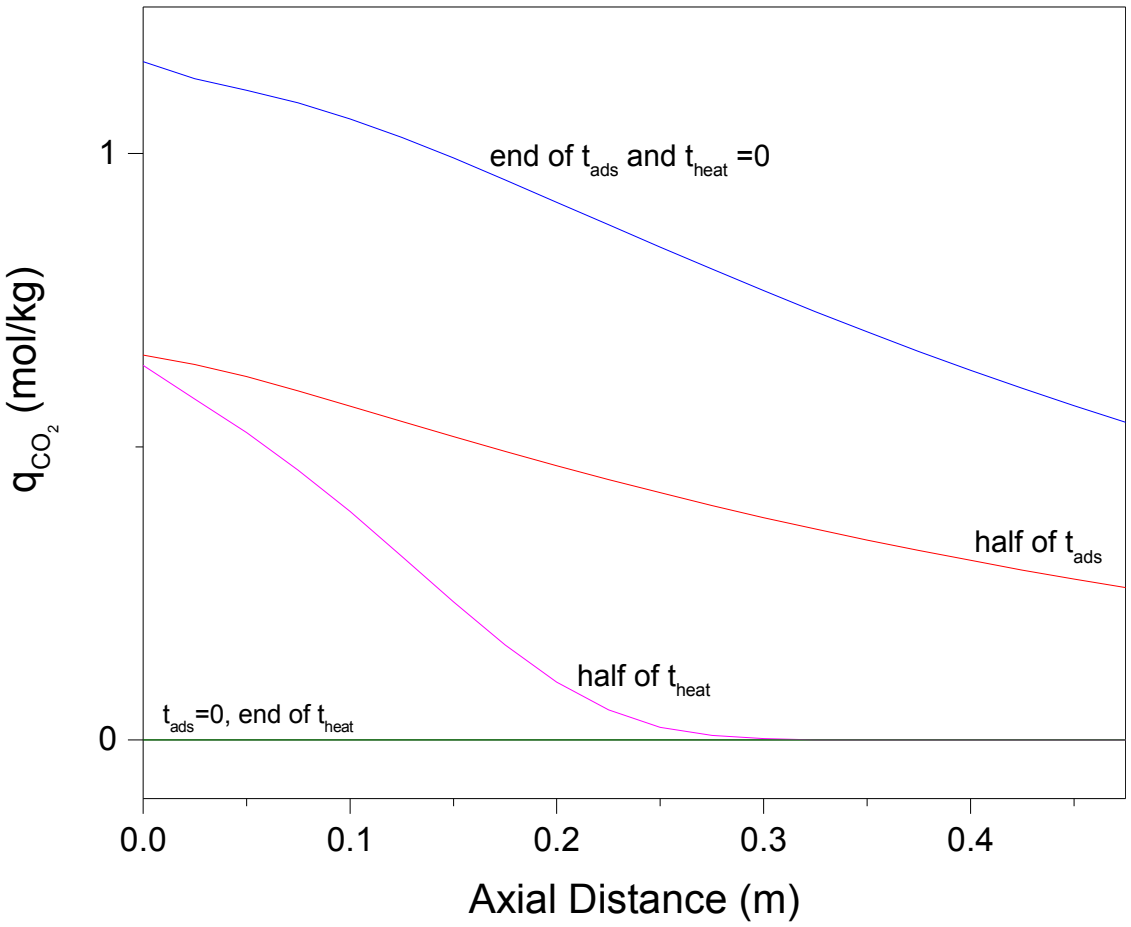

Figure C.2: Solid loadings across the bed at the end of each step in a 3-step TSA cycle for a 0.5m Bed